

UNIVERSITÀ POLITECNICA DELLE MARCHE
DIPARTIMENTO DI SCIENZE DELLA VITA E DELL'AMBIENTE

Corso di Laurea Magistrale in Biologia Marina



Applicazione di tecniche non invasive allo studio degli avvistamenti interannuali e dei moduli alimentari dello squalo balena *Rhincodon typus* nel Golfo di Tadjoura (Djibouti) e possibile relazione con le variabili ambientali

Application of non-invasive techniques to the study of interannual sightings and feeding behaviors of the whale shark *Rhincodon typus* in the Gulf of Tadjoura (Djibouti) and potential correlation with environmental variables

Relatore:

Prof.ssa Emanuela Fanelli

Correlatori:

Dr.ssa Francesca Romana Reinero

Laureanda: Rebecca Squadroni

Dr. Primo Micarelli

ANNO ACCADEMICO 2023/2024

SESSIONE ESTIVA

INDEX

ABSTRACT.....	2
1. INTRODUCTION	6
1.1 TAXONOMY	6
1.2 GEOGRAPHIC DISTRIBUTION.....	7
1.3 BIOLOGICAL FEATURES	9
1.4 FEEDING BEHAVIOR AND PREY ITEMS	11
1.5 ENVIRONMENTAL DRIVERS OF WHALE SHARK FEEDING BEHAVIOR AND DISTRIBUTION.....	16
1.6 THREATS AND CONSERVATION.....	22
1.7 THESIS OBJECTIVES.....	25
2. MATERIAL AND METHODS	26
2.1 STUDY AREA	26
2.2 DATA COLLECTION	28
2.3 I ³ S CLASSIC PHOTOIDENTIFICATION SOFTWARE.....	29
2.4 LASER-PHOTOGRAMMETRIC SURVEY	36
2.6 ENVIRONMENTAL DATA COLLECTION.....	41
2.7 DATA ANALYSIS.....	44
3. RESULTS	50
3.1 PHOTOIDENTIFICATION	50
3.2 LASER-PHOTOGRAMMETRIC SURVEY	50
3.3 SURFACE FEEDING BEHAVIORS.....	52
3.4 STATISTICAL ANALYSIS OF THE FEEDING BEHAVIOR OF WHALE SHARKS.....	54
3.4.1 CORRELATION MATRIX.....	54
3.4.2 MULTINOMIAL LOGISTIC REGRESSION MODEL	54
3.4.3 BEST SUBSET SELECTION (BSS).....	56
3.4.4 ODDS RATIO AND SAMPLE MARGINAL EFFECTS	57
3.4.5 CONFUSION MATRICES.....	58
3.4.6 ENSO AND INTERANNUAL SIGHTINGS OF THE WHALE SHARKS	63
4. DISCUSSION	65
4.1 PHOTOIDENTIFICATION	65
4.2 LASER-PHOTOGRAMMETRIC SURVEY	69
4.3 INFLUENCE OF ENVIRONMENTAL FACTORS ON FEEDING BEHAVIORS	70
4.4 INFLUENCE OF ENSO EVENTS ON THE FEEDING BEHAVIORS AND INTERANNUAL SIGHTINGS OF WHALE SHARKS IN DJIBOUTI.....	76
5. CONCLUSIONS.....	79
REFERENCES	81
ACKNOWLEDGEMENTS.....	105

ABSTRACT

Djibouti, in east Africa, is known to host an important seasonal feeding aggregation of whale sharks that allows frequent observation of their surface feeding behavior. From 2017 to 2024, 81 immature male whale sharks (*Rhincodon typus*) were photoidentified, confirming the importance of this area as a feeding ground for this species. During this period, immature males exhibited active, vertical, and passive surface feeding behaviors with different frequencies, as follows: in January 2017, the most observed was passive (54.91%), like January 2022 (44.56%); whereas in January 2020, vertical predominated (56.67%), mirroring November 2022 (49.49%) and January 2024 (53.69%). Surface feeding behaviors were affected by environmental factors, and chlorophyll-*a* was the main driver influencing the choice of the filter-feeding technique. Active and vertical feeding behaviors were favored by rainfall, lower sea surface temperature, worse sea conditions, and low wind speed during the morning; all factors positively correlated to chlorophyll-*a* concentration. On the contrary, passive feeding behavior was favored by opposite environmental conditions. Both passive and vertical feeding behaviors would occur during El Niño events, whereas active feeding is more common during La Niña events. Whale shark abundance and distribution are associated with food availability along coastal locations, where environmental conditions

support the species and zooplankton biomass. Furthermore, the El Niño Southern Oscillation (ENSO) phenomenon played a marginal role in influencing the interannual sightings of whale sharks in Djibouti over time, and other factors, which will be investigated in the future, could explain the number of sightings.

Keywords: whale shark, *Rhincodon typus*, feeding behaviors, environmental drivers

Lo squalo balena *Rhincodon typus* (Smith, 1828), il pesce più grande attualmente esistente, è un filtratore planctofago annoverato come “Endangered” nella Red List della IUCN (International Union for Conservation of Nature). È dunque di rilevanza vitale per la conservazione a scala globale di questa specie approfondirne l’abbondanza, la distribuzione e l’ecologia trofica. Le acque di Gibuti (Africa orientale) sono note per ospitare importanti aggregazioni stagionali di squali balena, consentendo la frequente osservazione in superficie sia degli esemplari che dei comportamenti alimentari esibiti.

A seguito delle Spedizioni scientifiche condotte dal Centro Studi Squali-Istituto Scientifico dal 2017 al 2024 a Gibuti, grazie all’utilizzo di metodologie non invasive come la fotoidentificazione e la laser-fotogrammetria, sono stati fotoidentificati 81 squali balena maschi immaturi, confermando l’importanza dell’area come zona di aggregazione per questa specie.

Per quanto riguarda i comportamenti alimentari dello squalo balena, il *vertical feeding* è stato il modulo più esibito e osservato nel gennaio 2020 (56.67%), novembre 2022 (49.49%) e gennaio 2024 (53.69%), mentre il *passive feeding* è stato il modulo più osservato nel gennaio 2020 (54.91%) e gennaio 2022 (44.56%).

La clorofilla-*a* è risultata la variabile ambientale con la maggiore influenza sui comportamenti alimentari, correlata a sua volta a tutti gli altri fattori ambientali

che ne influenzano la concentrazione. I comportamenti di alimentazione attiva e suzione (*active e vertical feeding* rispettivamente) che si manifestano principalmente in mattinata, sono favoriti generalmente da condizioni marine e climatiche avverse (precipitazioni, temperature superficiali del mare più basse, mare mosso e velocità del vento debole), le quali sono positivamente correlate alla concentrazione di clorofilla. Al contrario, il comportamento di alimentazione passiva (*passive feeding*) è favorito da condizioni ambientali opposte. Allo stesso tempo, i comportamenti di alimentazione passiva e suzione sembrerebbero manifestarsi durante gli eventi di El Niño, mentre quelli di alimentazione attiva durante gli eventi de La Niña.

Infine, il fenomeno di El Niño Southern Oscillation (ENSO) ha avuto un ruolo marginale nell'influenzare gli avvistamenti interannuali di squali balena a Gibuti nel corso del tempo. Altri fattori, omessi nel presente studio e che verranno investigati nel futuro, potranno far ulteriormente luce sul numero di avvistamenti di squali balena lungo le coste di Gibuti.

1. Introduction

1.1 Taxonomy

The whale shark *Rhincodon typus* (Smith, 1828) is the only member of the genus *Rhincodon* and belongs to the family Rhincodontidae within the order Orectolobiformes (Compagno, 2001; Fig. 1). This order comprises 42 species, belonging to seven families including Ginglymostomatidae (nurse sharks), Orectolobidae (wobbegongs) and Stegostomidae (zebra sharks) (Rowat, 2012).



Figure 1. Rhincodon typus (Smith, 1828).

Source: Andrea Izzotti

1.2 Geographic distribution

Whale sharks inhabit all tropical, subtropical, and warm temperate seas. Hitherto, this species was believed not to be present in the Mediterranean Sea, although recent sightings have confirmed its first observation there as well (Turan *et al.*, 2021; Fortič *et al.*, 2023). Whale sharks predominantly dwell in coastal, oceanic, and epipelagic waters (up to 200 m of depth), but they regularly undertake very deep (“extreme”) dives (>500 m) (max. depth recorded 1,928 m) likely due to foraging events within the deep scattering layer (Tyminski *et al.*, 2015).

Aggregations of *R. typus* are seasonally documented in specific hotspot areas, showing a higher degree of site fidelity (Fig. 2): from October to February, whale sharks aggregate in Djibouti (Micarelli *et al.*, 2017; Boldrocchi *et al.*, 2020; Di Capua *et al.*, 2021), Tanzania (Rohner *et al.*, 2015), South Africa (KwaZulu-Natal), and Australia (Christmas Island); from March to May, in Belize (Gladden Spit), India (Gujarat), Australia (Ningaloo Reef), and the Philippines (Sequeira *et al.*, 2012); between late July and mid-August, off of Isla Holbox in the Yucatán Peninsula of Mexico (de la Parra Venegas *et al.*, 2011); from June to October, in Indonesia (West Papua) (Marliana *et al.*, 2018); from August to October, in Portugal (Azores), Mozambique, Seychelles, South and North Gulf of California, and North Gulf of Mexico (Rowat and

Brooks, 2012); in November and December, in Nosy Be (Madagascar) (Bava *et al.*, 2022; Marsili *et al.*, 2023); and from December to May, in the Maldives (Ari Atoll) (Riley *et al.*, 2010). These aggregations are thought to be linked to zooplankton prey density and abundance and to environmental factors strictly correlated among them, like chlorophyll-*a* concentration and sea surface temperature (SST), rather than socially driven interactions (Colman, 1997). However, most of the sharks observed aggregating at the surface in these areas are immature males, and it is rare to find both immature and mature females, new-born whale sharks or samples smaller than 3 m or larger than 10 m in total length (TL), indicating that studies focusing on immature male-based aggregations cannot fully represent the entire population of whale sharks (Robinson *et al.*, 2017).

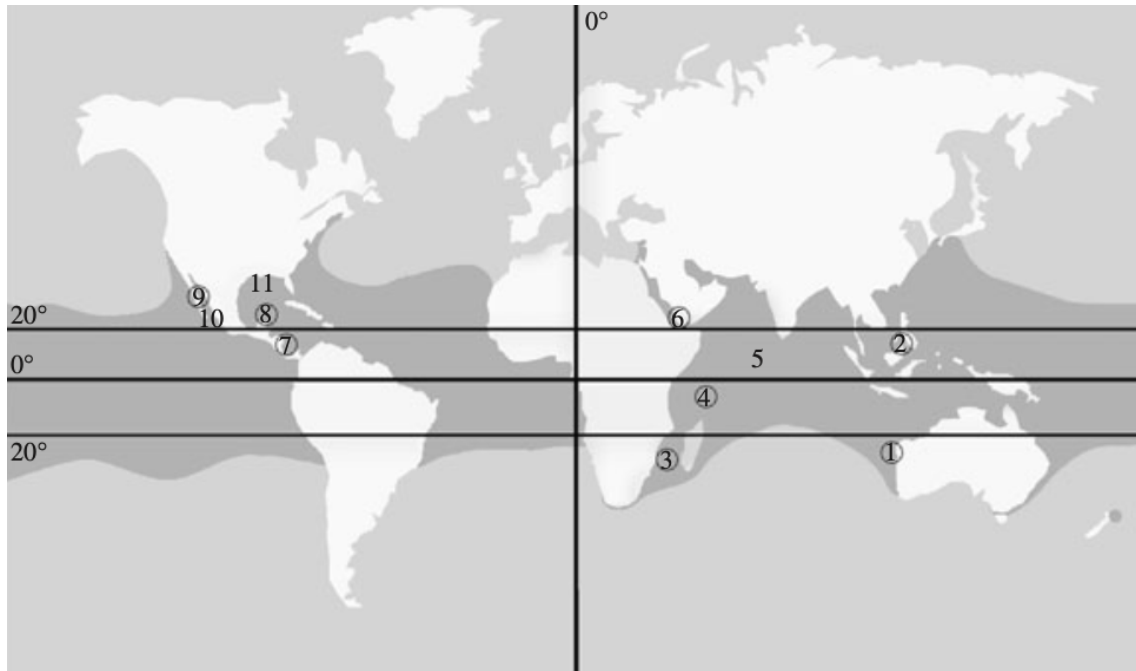


Figure 2. Global range of *R. typus* distribution with the main aggregation areas: 1, Ningaloo; 2, Philippines; 3, Mozambique; 4, Seychelles; 5, Maldives; 6, Djibouti; 7, Belize; 8, Holbox; 9, North Gulf of California; 10, South Gulf of California; 11, North Gulf of Mexico. The circled hotspots indicate the sites of tourism activities of *R. typus*.
Source: Rowat and Brooks (2012)

1.3 Biological features

The whale shark is the world's largest living fish species of all time, with the largest known specimen recorded being 20 m long and 34 tons in mass from Taiwan (Chen *et al.*, 1997). *Rhincodon typus* is characterized by a broad, flat head with a large terminal mouth, modified gill rakers, and a unique pattern of the skin with light spots and stripes over a dark background (Compagno, 2001). The evolutionary advantage of this pattern, which represents a “fingerprint” to distinguish specimens, has not been investigated. Multiple theories have been

reported indicating the use of this skin pigmentation to camouflage with the surrounding waters acting as a disruptive coloration, or to provide protection against ultraviolet radiation to which this species is exposed by staying most of the time in surface waters (Becerril-García *et al.*, 2021), or may be useful for individual recognition between conspecifics (Martin, 2007).

In addition, *Rhincodon* refers to the "rasp-like teeth" of the whale shark, one of the numerous distinctive characteristics of the species (Dove and Pierce, 2022; Fig. 3). Despite having minute and numerous teeth, whale sharks are planktivorous and filter-feeder animals and teeth probably represent a vestigial trait, meaning that these are residual features from evolutionary adaptation and are no longer functional in the feeding process (Rowat, 2012; Taylor, 2007).



Figure 3. Rhincodon typus dentition.

Source: sharkguardian.org

1.4 Feeding behavior and prey items

Despite studies have demonstrated that whale sharks feed on zooplankton that tends to aggregate in dense patches (Rohner and Prebble, 2021), stable isotopes, zooplankton taxonomic analysis, and visual observations, suggest that the diet of whale sharks change as they increase in size, from smaller zooplankton prey such as holoplanktonic organisms (Copepoda, Chaetognatha, Ostracoda, Thaliacea, Amphipoda, Pteropoda, and Sergestidae) and meroplanktonic organisms (Bivalvia, Gasteropoda, Polychaeta, Cirripedia and Malacostraca larvae, Teleostei eggs and larvae), to schooling fishes such as sardines, anchovies, mackerels, and occasionally larger prey such as small tunas, albacores, and squids (Colman, 1997; Motta *et al.*, 2010; Boldrocchi and Bettinetti, 2019; Montero-Quintana *et al.*, 2021; Diamant *et al.*, 2021; Bava *et al.*, 2022; Marsili *et al.*, 2023). In fact, recent studies in Nosy Be (Madagascar) highlighted that the biomass of zooplankton sampled in this specific area was two orders of magnitude lower than the minimum energy requirements of juvenile whale sharks. Hence, it was not energetically sufficient to sustain young specimens alone, suggesting the possibility that they feed not only on zooplankton but also on multiple prey sources such as tunas, anchovies, and mackerels, which could be the primary target of whale sharks (Bava *et al.*, 2022; Marsili *et al.*, 2023). Moreover, smaller sharks are seen along coastal

areas while larger sharks are rarely observed, suggesting that adult sharks may be more specialized and may have advantages in foraging at depths where the zooplankton aggregations are smaller and less dense (Rohner and Prebble, 2021).

One of the peculiarities of *R. typus* is the fact that it lives and feeds in warm waters where plankton productivity is lower compared to other planktivorous shark species habitats (Rohner and Prebble, 2021). Unlike the filtering apparatus of the other filter feeding sharks, the basking shark (*Cetorhinus maximus*) and the megamouth shark (*Megachasma pelagios*), *R. typus* feeds by suction and this technique may allow it to capture a wider range of prey (Nelson and Eckert, 2007). This technique is however energetically expensive for whale sharks, as the hydrodynamic profile is broken by the open mouth, leading to an increased drag. In fact, whale sharks only feed when the biomass of the prey present is abundant enough to have an energy gain (Rohner and Prebble, 2021). When feeding, planktonic prey are captured by filtering the sea water, which passes through a specialized apparatus comprising five sets of porous pads on each side of the pharyngeal cavity. The pads are supported by primary and secondary cartilaginous vanes, that direct the water across the gill filaments.

The water is then expelled through the gill slits, while the retained preys become a source of nutrition (Motta *et al.*, 2010; Fig. 4). The mechanism of filtration of food particles in whale sharks varies depending on their maturity, due to the development of their

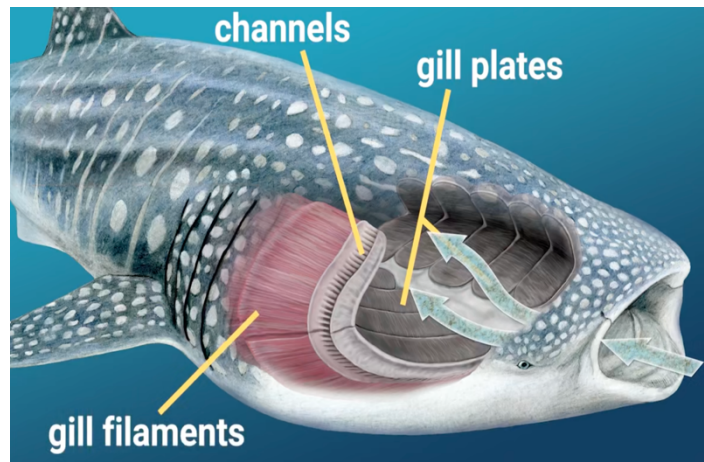


Figure 4. *Filter feeding mechanism of R. typus.*

Source: nationalgeographic.org, illustration by Emily S. Damstra

filtration system (Paig-Tran and Summers, 2011). Adult whale

sharks predominantly feed through a form of cross-flow filtration (Motta *et al.*, 2010). In contrast, smaller neonate sharks collect particles in their esophagus, as their filtration system is not yet fully developed (Paig-Tran and Summers, 2011).

To ingest the highest possible amount of prey and to spend the lowest amount of energy, the whale shark has developed three specific surface filter-feeding strategies, depending on the density of zooplankton in the water: *ram (or passive)-feeding* (or simply passive), *vertical feeding* (or simply vertical), and *active surface ram-feeding* (or simply active) (Nelson and Eckert, 2007; Fig. 5).

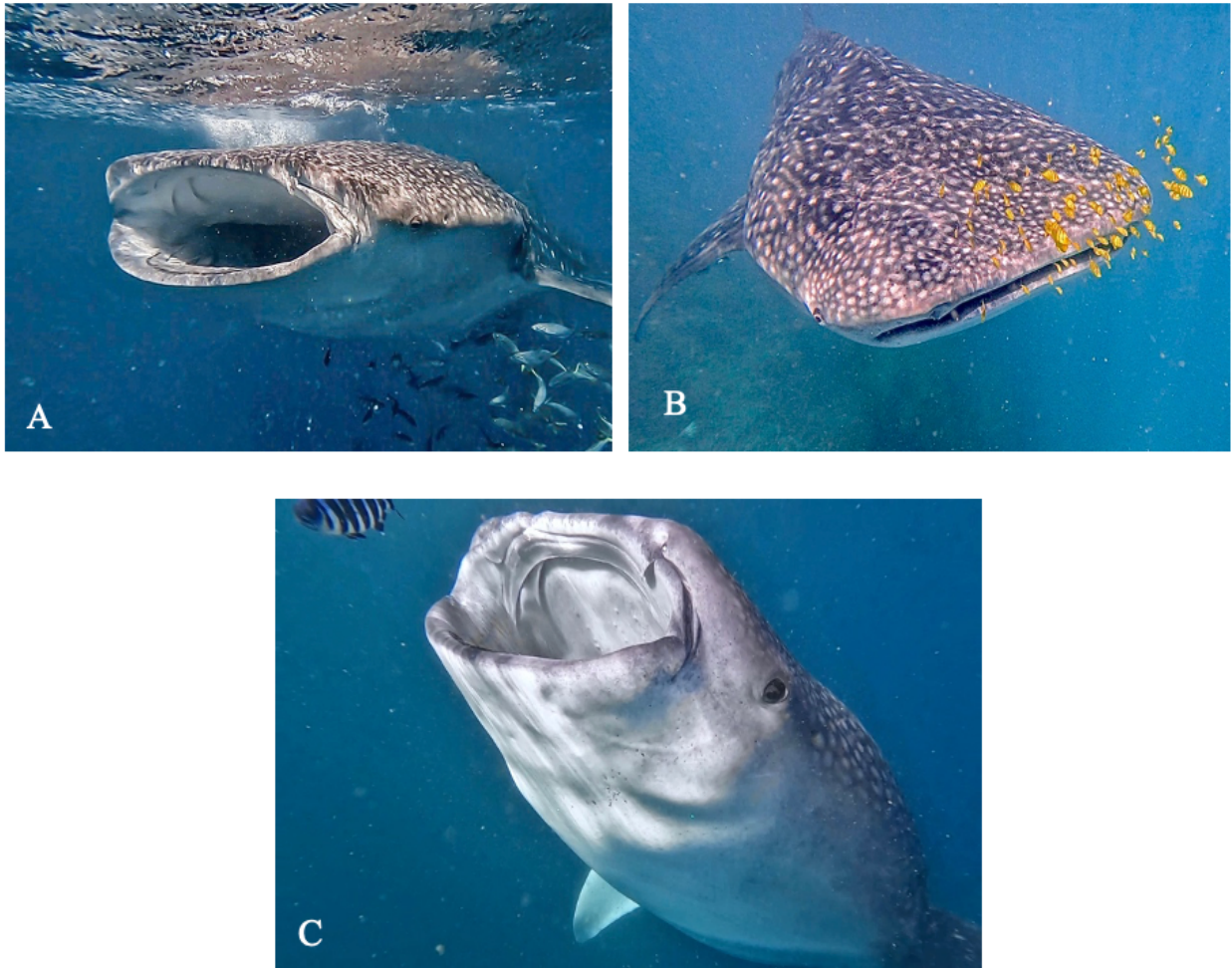


Figure 5. Whale shark feeding behaviors: (A) *active surface ram-feeding*; (B) *ram (or passive)-feeding*; (C) *vertical feeding*.

Source: Photo by Rebecca Squadroni, Djibouti 2024.

The predominant method of filter feeding observed in whale sharks, as documented in existing literature, is active (Nelson and Eckert, 2007; Motta *et al.*, 2010) (Fig. 5A), which occurs when the zooplankton density is high and the shark feeds directly at the surface, swimming actively in a forward motion using both suction and ram feeding techniques to catch the prey, with the upper

jaw, the head, the first dorsal fin, and the upper caudal fin penetrating the sea surface and swimming patterns involving head and body direction changes.

The first documentation of whale shark active feeding was recorded in the Bahamas by Gudger (1941a) and, since then, several observations occurred, such as in Yucatán, Mexico, where a study led by Cade *et al.* (2020) revealed that three out of four feeding whale sharks exclusively employed this active feeding method for over 90% of the 30 logged hours of observed feeding behavior.

Instead, with low zooplankton densities, the most prevalent feeding technique is passive (Nelson and Eckert, 2007) (Fig. 5B), in which whale sharks swim slowly in circular or S-shaped patterns just below the surface, using a ram feeding technique with the mouth from halfway to wide open, getting the water passing into the mouth and through the gills, without doing gulping or suction feeding (Taylor, 2007; Rowat and Brooks, 2012).

On the contrary, the least energetically demanding surface feeding behavior is vertical (Cade *et al.*, 2020) (Fig. 5C), when zooplankton density is medium and whale sharks' body position is almost vertical, with little or no forward movement and with the mouth directed toward the surface, gulping water using a suction technique, and expelling water out the gills slits. This behavior has been observed for the first time along the Cuba coast by Gudger (1941a) and is

commonly recorded in the “Afuera” aggregation of the Mexican Caribbean, where whale sharks are called “botella”, due to their resemblance to an empty bottle floating upright on the surface (De la Parra Venegas *et al.*, 2011; Dove *et al.*, 2022).

A similar trend between surface filter-feeding techniques and zooplankton prey abundance was also observed by Di Capua *et al.* (2021) in Djibouti, where passive feeding activity was recorded during the lowest abundance of zooplankton, while vertical and active feeding activities occurred during the highest one.

1.5 Environmental drivers of whale shark feeding behavior and distribution

Flexibility for changing feeding behaviors is related to the availability of prey, and surface currents or chlorophyll-*a* concentration can indirectly affect the distribution of prey by influencing their behavior, movement, and abundance (Sleeman *et al.*, 2010). Moreover, this species maximizes its feeding efficiency by seeking patches of high concentration of prey instead of exhibiting prey selectivity due to constant changing environmental factors (Whitehead, 2020). Several studies have described the influence of some environmental factors on whale sharks’ movement pattern, sightings, and coastal aggregation (Sleeman

et al., 2010; Rohner *et al.*, 2013; Hacothen-Domené *et al.*, 2015; Ranintyari *et al.*, 2018; Manuhutu *et al.*, 2021). However, the effects of environmental factors on surface feeding behaviors and on the choice of a filter-feeding technique rather than another, have never been described in the literature.

Previous investigations in Djibouti found a positive correlation between chlorophyll-*a* concentration and zooplankton biomass (Boldrocchi *et al.*, 2020) and an increase of both at the end of the summer season. Indeed, from July to September, southwest monsoon winds moving eastward enhance upwelling and, consequently, cooler SST in the Gulf of Tadjoura (Omar *et al.*, 2016) increasing the chlorophyll-*a* concentration and zooplankton biomass. The opposite trend occurs during winter with northeast monsoon winds inducing surface water flowing toward the Gulf of Tadjoura, reducing the upwelling (Omar *et al.*, 2016; Boldrocchi *et al.*, 2020).

Furthermore, Motta *et al.* (2010) observed in Cabo Catoche (Mexico) that whale sharks approached the surface to filter feed during early morning with a peak in abundance during mid-morning, returning to slightly deeper water around noon, and resurface to feed in the afternoon and to deep waters again in late afternoon, showing ram filter feeding techniques when swimming between 0 and 1 m depth in the daytime. On the contrary, Gleiss *et al.* (2013) stated that whale sharks at Ningaloo Reef (Western Australia) exhibited ram filter feeding

techniques primarily during sunset and the first hours of night, whereas vertical movement peaked prior to them.

Surface feeding behaviors and the distribution range of whale sharks are also strongly affected by water temperature: SST plays a crucial role in the feeding behavior of whale sharks by influencing food availability, migration patterns, metabolic rates, and behavioral responses (Arrowsmith *et al.*, 2021; Sequeira *et al.*, 2013). The warming of oceans has become an undeniable reality: as SSTs rise, so do the boundaries of suitable habitats for whale sharks, which could trigger a redistribution of these creatures. The consequences regarding the impact of warming seas on the distribution of *R. typus* have already been documented (Sequeira *et al.*, 2013). For instance, there have been sporadic sightings of individuals at higher latitudes than their typical range (30°N-35°S), specifically in the Bay of Fundy, Canada (Turnbull and Randell, 2006), in the north-eastern part of New Zealand (Duffy, 2002) and in the southern Azores, Portugal, probably in response to the warming of the waters (Afonso *et al.*, 2014). In addition, SST can influence the metabolic rates of marine organisms, including whale sharks, which seem to avoid high temperatures (Sequeira *et al.*, 2013). Indeed, warmer temperatures may increase metabolic demands, potentially affecting their energy requirements and feeding behavior. Consequently, they may need to consume more food to sustain their energy

needs or adjust their feeding strategies in response to changes in SST (Sequeira *et al.*, 2014).

Moreover, whale sharks can regulate their body temperature and optimize their thermal environment in response to changing conditions in the ocean by combining horizontal migrations with vertical movements (Arrowsmith *et al.*, 2021). Ectotherm species like *R. typus*, in fact, have the necessity to warm up in surface waters by basking at sunlight and then descend to deeper, colder waters to maintain their thermal equilibrium. According to Arrowsmith *et al.* (2021), when the SST exceeds the optimal range (24°C – 30°C), whale sharks alter their behavioral strategies anticipating feeding events and adjusting their diving patterns to sustain themselves, highlighting the crucial role of SST in foraging patterns and thermoregulatory behavior.

Future climate forecasts, referred to a relatively short time frame (i.e., 80 years), not only indicate a weak but noticeable poleward shift of habitat, particularly evident in the Atlantic and Indian Oceans, but also a general contraction of suitable habitats, particularly in the equatorial region (Sequeira *et al.*, 2014). These global predictions are consistent with forecasts for zooplankton biomass (Beaugrand *et al.*, 2009) and many other marine species (Dulvy *et al.*, 2008). However, whale sharks may face greater challenges in adapting to the new

environmental conditions, given their extended lifespan and delayed maturity (Báez *et al.*, 2019).

Another relevant environmental factor influencing the global distribution of whale sharks is the El Niño Southern Oscillation (ENSO) phenomenon. ENSO events can determine variations in SSTs, winds' direction and speed, rainfall, and sea conditions, driving global climate fluctuations across seasonal to interannual time scales (Wolter and Timlin, 2011). During El Niño events, SSTs in the eastern Pacific Ocean tend to rise, leading to changes in atmospheric circulation patterns causing trade winds to reverse towards the southeast. In addition, El Niño affects weather conditions causing heavy rainfalls and flooding in South America and droughts in Australia and Southeast Asia (Wolter and Timlin, 2011). Under typical circumstances, upwelling processes facilitate the movement of cold, nutrient-rich water from the ocean depths to the surface. However, during El Niño events, this upwelling weakens or halts entirely. Consequently, the reduction in nutrient availability disrupts the proliferation of phytoplankton along the coast, triggering a cascading effect on marine ecosystems and organisms depending on it, including the whale shark (Wolter and Timlin, 2011). Conversely, during La Niña events, when SSTs in the eastern Pacific are cooler than average, the trade winds and upwelling intensify, bringing nutrients availability along the western

coast of America (Wolter and Timlin, 2011). This increased productivity can have positive effects on marine ecosystems, benefiting various marine organisms, including those higher up in the food web, such as the whale shark. According to Wilson (2001), the number of sightings of whale sharks in Ningaloo Reef (Australia) was greater during La Niña events compared to El Niño years. The author suggested that this difference may be linked to variations in ocean currents, where weak water currents during El Niño events result in reduced food availability and, consequently, fewer shark aggregations. Contrarily, stronger currents during La Niña events lead to an increase in shark sightings in response to a greater abundance of food sources (Wilson, 2001). Likewise, the study of Sleeman *et al.* (2010) reported that both the Southern Oscillation Index (SOI) and wind shear variables have a positive correlation with the abundance of whale sharks in Ningaloo Reef. Specifically, a higher number of whale sharks is observed during periods of stronger Southern Oscillation, indicating La Niña conditions, where alterations in ocean currents and SSTs might affect the migration patterns of whale sharks. Similarly, the wind-driver upwelling could impact the availability of prey for *R. typus* by affecting productivity changes in the ecosystem.

1.6 Threats and conservation

Like many other elasmobranchs, the whale shark exhibits a K-strategy with low fecundity, slow growth rates, late sexual maturity, and extended longevity (*sensu* Colman, 1997) that make this species susceptible to overexploitation (Rohner *et al.*, 2015). Given these features and despite there are some hotspots around the world, it is imperative to recognize the multiple threats they face. Whale sharks are not only threatened by direct human actions, but they are also increasingly vulnerable to the impacts of environmental shifts. Therefore, *R. typus* is currently categorized as “Endangered” in the IUCN Red List (Pierce *et al.*, 2016) and included in several international conventions and agreements, as in Appendix II of the *Convention of Migratory Species of Wild Animals* (CMS) since 1999 and Appendix II of the *Convention on International Trade of Endangered Species* (CITES) since 2002.

Since 1990, ecotourism of whale sharks has rapidly increased, resulting in positive impacts on local economies, conservation efforts, and public awareness of marine biodiversity if it is managed carefully to minimize negative effects on the animal and its feeding behavior (Rowat *et al.*, 2012). However, the frequent disregard of the code of conduct by tourists has led to a decrease in the number of *R. typus* present at the aggregation sites. These interactions can have effects both in the short and long term. Short term effects

include barking, rapid diving, and avoidance feeding behaviors, which have been observed in Ningaloo Reef, Australia (Norman, 2002). Long-term effects, on the other hand, may include stress, avoidance, or displacement (Rowat *et al.*, 2012). However, these observations contrast with the behaviors observed in whale sharks in Oslob, Philippines, where sharks are provisioned daily, showing an ability to modify their feeding behavior in response to anthropogenic stimuli and being less likely to exhibit avoidance (Legaspi *et al.*, 2020).

As whale sharks spend most of their time on the surface of coastal feeding areas, they are particularly vulnerable to vessel strikes, which are unlikely to be documented (Speed *et al.*, 2008). Furthermore, this species undertakes annual long-distance migrations linked to prey density and abundance across both international and national waters. Some of them are ensured by legislation and management, while others do not offer protection and, instead, exploit *R. typus* for their meat, fins, and other products (Womersley *et al.*, 2022). In addition, as whale sharks represent an indicator of tuna presence, they are often caught as bycatch in gillnets, purse seine nets, and other types of fishing gear that are primarily set to catch other target species like tropical tuna (Báez *et al.*, 2019). Moreover, although pollution hasn't been widely acknowledged as a primary threat to the survival of whale sharks, its negative impact could

influence the feeding behavior of this species (Marsili *et al.*, 2023). Recent analysis revealed the consistent presence of pollutants such as HCB, DDT, and PCBs in zooplankton samples in the Gulf of Tadjoura (Djibouti; Boldrocchi *et al.*, 2018), Ningaloo Reef (Australia), and Madagascar (Marsili *et al.*, 2023). In fact, persistent organic pollutants (POPs) discharged into marine environments enter the food web and are absorbed by organisms from the lowest trophic level, such as zooplankton, to the ones of highest trophic levels, such as whale sharks, which bioaccumulate and biomagnify (Boldrocchi *et al.*, 2018).

Beyond these direct threats, there is also growing concern that climate change may already be impacting whale shark surface feeding behaviors (Sequeira *et al.*, 2014). While the direct impacts of climate change on whale sharks may be limited, the indirect effects through alterations in their habitat, food availability and densities, and ecosystem dynamics represent a significant challenge to their survival and conservation efforts. Tropical marine ecosystems, renowned for their rich biodiversity and complex food webs, are particularly vulnerable to the effects of climate change. Studies have shown that shifts in ocean temperature, alterations in nutrient availability, and changes in oceanographic processes can have far-reaching consequences, such as loss of habitat, a decrease in oxygen concentrations, acidification, and an increased seawater temperature (Báez *et al.*, 2019). In this context, climate change can alter the

distribution and productivity of planktonic prey, potentially affecting the surface feeding behavior and migration patterns of whale sharks and leading to food shortages in feeding grounds (Jaramillo *et al.*, 2023). Nevertheless, alterations of suitable areas for whale sharks do not necessarily guarantee the occurrence of new zooplankton blooms within these regions (Báez *et al.*, 2019).

1.7 Thesis objectives

Within this framework, given that climate change can alter the distribution and productivity of planktonic prey, potentially affecting the surface feeding behavior and abundance of whale sharks, and considering the threatened situation they face at their coastal aggregation sites due to shore-based fishing and boating activities, it is fundamental to understand the drivers of their filter-feeding strategies in the conservation management of this species. Thus, the aims of this study are: (1) to utilize non-invasive techniques for the identification and measurement of sighted whale sharks; (2) to describe the surface feeding behaviors of the whale shark at Djibouti aggregation area across years, and (3) to investigate the main environmental drivers of such behaviors.

2. Material and Methods

2.1 Study area

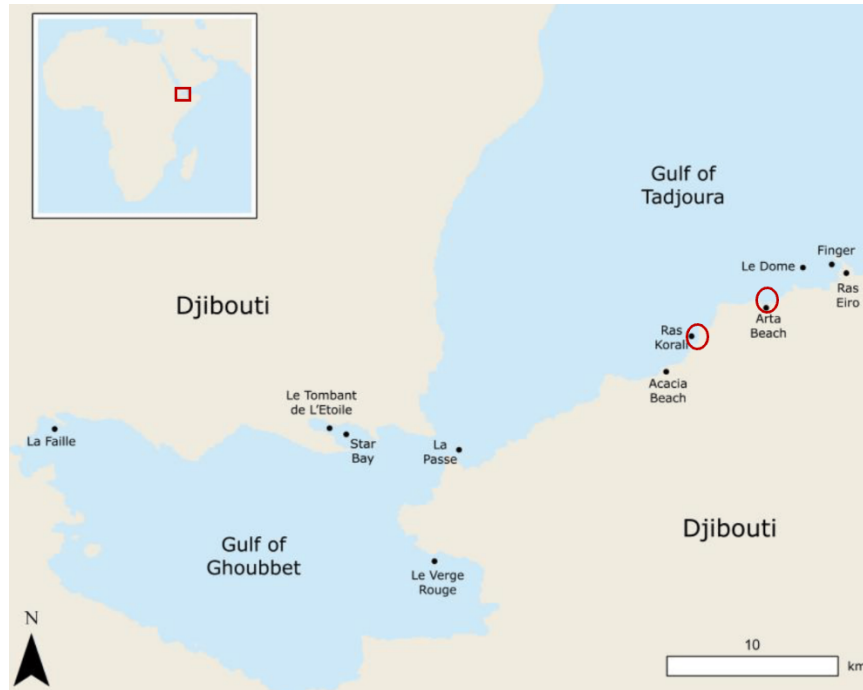


Figure 6. Djibouti (Africa) and the study areas of Arta Beach and Ras Korali, within the Gulf of Tadjoura (red dots).

Source: Boldrocchi *et al.* (2023)

Five scientific expeditions (January 2017, January 2020, January 2022, November 2022, and January 2024) aimed at the study of the ecology and ethology of whale sharks were carried out by the Sharks Studies Center-Scientific Institute of Massa Marittima (GR) in Djibouti, located in the Horn of Africa and bordered by Eritrea on the north, Somalia on the south, Ethiopia on the southwest, and the entrance of the Red Sea on the east (Fig. 6).

Observations were specifically conducted in Arta Bay (11°35'38,4" N, 42°49'37,0" E) and Ras Korali (11°34'27,7" N, 42°46'24,1" E).

The climate in Djibouti is desertic, dry, and tropical. Temperatures are consistently high throughout the year, with an average mean temperature of 28.50 °C, and the sea surface temperature is between 25°C and 28°C (Copernicus.eu). Rainfall is low and irregular, amounting to 224.52 mm annually, typically occurring during three monsoonal rainy seasons that are influenced by El Niño Southern Oscillation (ENSO), with lower rainfall during El Niño years and greater rainfall during La Niña events (www.climateknowledgeportal.worldbank.org). The SST is between 25°C and 28°C (Copernicus.eu).

The Gulf of Aden is strongly influenced by Indian Monsoon. During the winter months, typically between December and February, northerly winds give rise to a northern anticlockwise gyre. On the contrary, during summer, the southwest monsoon prevails, which enhances the eastward movement of surface water and induce upwelling (Boldrocchi *et al.*, 2020).

Within the Gulf of Aden, on the coastline of Djibouti, lies the Gulf of Tadjoura (Fig. 6, right image) where the seabed slopes steeply from the gulf's shore, reaching a depth of around 100 m at 2 km offshore and 450 m at its center. This site represents an important migratory stage for whale sharks, which seasonally

aggregate from October to February, especially juvenile males (Boldrocchi *et al.*, 2020), making it an ideal location to study the ecology and the ethology of this species and the influence of environmental factors on their surface feeding behavior.

2.2 Data collection

The fieldwork took place during January in 2017, 2020, 2022, and 2024. In 2022, a second expedition in November was carried out.

During all these years, the research team stayed aboard the sailboat “Elegante” (Fig. 7). Upon anchoring, two Zodiacs were simultaneously engaged to search for whale sharks by observing their dorsal fin or the upper lobe of the caudal fin visible above the sea surface, or by identifying vortex patterns on the water when suction feeding just beneath the surface (Boldrocchi *et al.*, 2020).



Figure 7. Sailboat "Elegante" where the fieldwork took place.

Source: Sharks Studies Center-
Scientific Institute

Each research team member was equipped with essential snorkeling gear, such as a mask, snorkel, fins, and action-camera. Once a specimen was spotted, the team approached the shark at a safe distance, getting into the water slowly and quietly to avoid disturbing the individual. While swimming underwater next to it, photographs and videos of its left and right sides and scars or unique signs used to identify the animal were taken, and the sex of each shark was determined by observing the presence of claspers between pelvic fins for males or their absence for females (Boldrocchi *et al.*, 2020). In addition, two research team members used the laser-photogrammetry survey to assess the total length (TL) of whale sharks.

The research consisted of two daily excursions, scheduled as follows: from 9.00 to 12.00 and from 14.00 to 17.00. After each trip, research team members analyzed photos and videos collected, recording information on sex as well as the ID number of the shark, date and position of sighting. In the comment section, both the surface feeding activity of the animal and marks and wounds were recorded to create an identification sheet for every sighted shark.

2.3 I³S Classic photoidentification software

Like “human fingerprints”, whale sharks have a unique dorsal pattern of white spots and stripes on a dark background that presents only minor changes over

the years (Arzoumanian *et al.*, 2005). This allows each individual to be photoidentified, providing an estimation of population size and distribution through digital programs like the I³S *Classic* (Arzoumanian *et al.*, 2005; Brooks *et al.*, 2010). The use of natural markings characteristic of the species (scars, scratches, etc.) can also make it easier to recognize sharks (Boldrocchi *et al.*, 2020).

Photoidentification is a non-invasive technique that allows the use of just an action-camera to take photos or videos, and whale sharks are one of the best examples on which this technique can be applied, also because they are calm and easy to approach when taking videos and photos in snorkeling activities (Arzoumanian *et al.*, 2005).

The I³S *Classic* (Interactive Individual Identification System) photoidentification software uses photographs of the skin pattern behind the fifth gills of both sides of the shark to compare the frames acquired with the ones already loaded in the database in order to find a match between them and see if the shark has been previously photographed (Van Tienhoven *et al.*, 2007). This photoidentification program is adapted from an algorithm developed within the astronomical community for stellar pattern recognition (Arzoumanian *et al.*, 2005) and four different versions (I³S *Classic*, I³S *Pattern*, I³S *Contour*, and I³S *Spot*) are available depending on the pattern to be

recognized or matched (Speed *et al.*, 2007). All programs work in a similar way and help the operator to highlight the pattern of animals and to compare it to the ones present in the database: if the software finds a match, the animal is already present in the database; if there is no match, the individual is new and can be added to the database (Arzoumanian *et al.*, 2005).


By using this advanced image processing software, a database of known whale sharks has been created by the Sharks Studies Center-Scientific Institute starting from the first expedition conducted in 2017 between Djibouti and Madagascar, aiding population monitoring, research, and conservation efforts for this species.

The protocol for data collection and processing images through the I³S *Classic* was as follows:


1. All videos of whale sharks were reviewed and analyzed based on the day of sighting and the number of specimens. Then, the best frame of both sides of the animal representing the area between the fifth gill slit and the pectoral fin was selected, as this area exhibits minor changes over the years (Arzoumanian *et al.*, 2005).
2. The extrapolated frame was uploaded on the I³S *Classic* program for identification, verifying whether the individual has already been inserted in the database (resighting) or was new sighting.

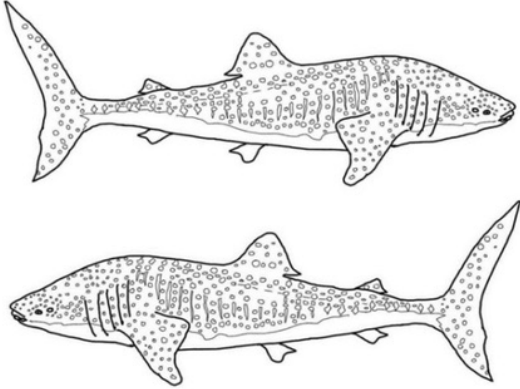
- For each new individual, an identification sheet was filled out indicating the specimen identification number (the same number used in the I³S database), the left and/or right frames used for photoidentification, date, time, and location of the sighting, sex and TL (either assumed or assessed by laser-photogrammetry), any potential scars or distinctive marks visible from the footage, and the different feeding behaviors (Fig. 8).

Rhincodon typus Smith, 1828			
Left side		Shark ID	
Right side			
Date	N°	Length	Sex
GPS			
Video references			
Photo references			
Comments			



Body marks





X=Scars O=Others

Figure 8. Model of whale shark identification sheet.

Source: Sharks Studies Center-Scientific Institute

The I³S *Classic* software employs a reference system comprising three blue points chosen for pattern input that can be easily marked in every photograph, known as “fingerprints”: the point at the top of the fifth gill slit (top 5th gill), the lower point of the fifth gill slit (bottom 5th gill), and the marginal point at the end of the pectoral fin (pectoral fin). Then, the operator manually selects the most representative white spots within the reference area, marking the center of each one in red. In order to make a reliable comparison, it is necessary to insert 12-20 red points (Fig. 9) so that the image can be processed and compared with the others in the database (Van Tienhoven *et al.*, 2007).



Figure 9. Data output from I³S *Classic* of a whale shark (number 18) in Djibouti (2024). The three reference points are highlighted in blue, and the red spots of the two-dimensional pattern are marked for comparison with other sharks.

Source: Sharks Studies Center-Scientific Institute

Once the frame is saved in the database, the I³S *Classic* program assigns a score to the match (Fig. 10). The lower the score, the greater the similarity between the individuals. A recognition score of 0.00 represents a perfect match between the new individual and one already present in the database (resighting); a score ≤ 10.00 indicates a reliable match, suggesting that the animal is the same; a score ≤ 20.00 requires the operator to visibly compare the two frames to verify whether it is the same shark or a new one; if the score is ≥ 20.00 , is not considered.

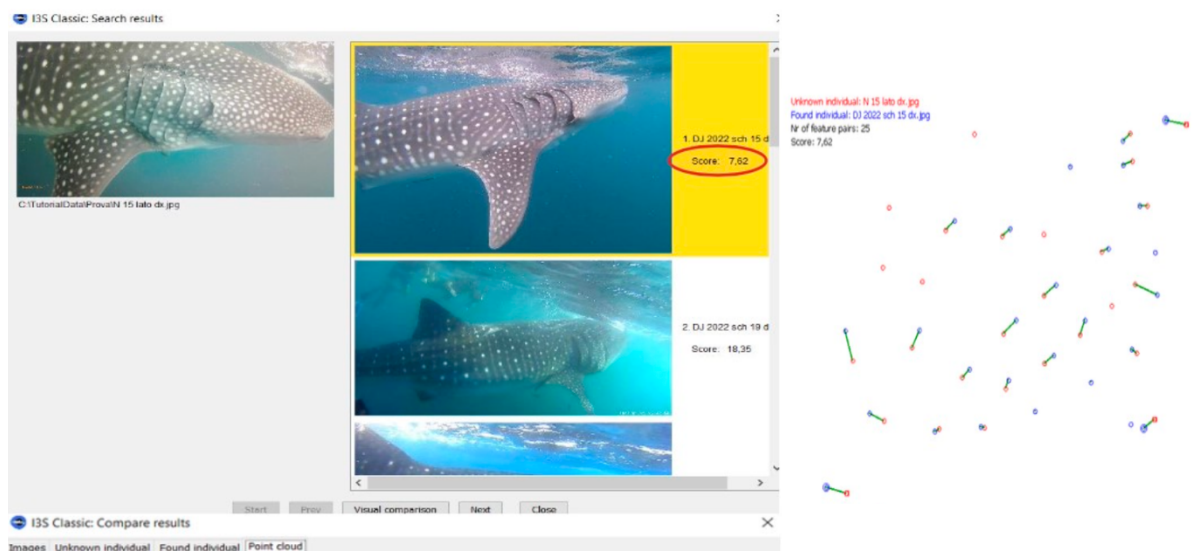


Figure 10. Comparison of different frames of whale sharks with the I³S *Classic* software. The score is 7.62 between the two photos, suggesting that the animal is the same, thus indicating a reliable match.

Source: Sharks Studies Center-Scientific Institute

According to the results, if the individual is determined to be new based on the score and comparison process, it is included in the identification database. On the contrary, if the individual is recognized as previously recorded, it is not added to the database but rather categorized as a resighting.

Although I³S *Classic* has been shown to be efficient, potential low errors (4-5%) can arise from filming moving animals underwater. There are some limitations to be considered:

- The software applies a 2D model to a 3D animal. As observation angles increase, the limitations of the 2D approach become more evident.
- The animal's structure is not linear, meaning that the body parts do not maintain a consistent position relative to each other, particularly the pectoral fin that can cover the identification area.
- The frame can be altered by the reflection of sunlight, air bubbles, and other individuals swimming around the shark.

Consequently, it is important to configure the camera with a narrow angle, perpendicular to the identification area, to prevent distortion of the animal's structure. Moreover, the presence of the same operator working on the identification is crucial for an accurate result, avoiding errors such as a corresponding image file saved in the software.

2.4 Laser-photogrammetric survey

Laser-photogrammetry system is the second non-invasive methodology used for the measurement of the TL of every sighted whale shark. The equipment consists of an underwater action camera placed on a rigid horizontal plane with two parallel green lasers positioned on either side at a fixed distance of 30 cm (Fig. 11). The color of the laser used must be green because it is easily visible underwater.

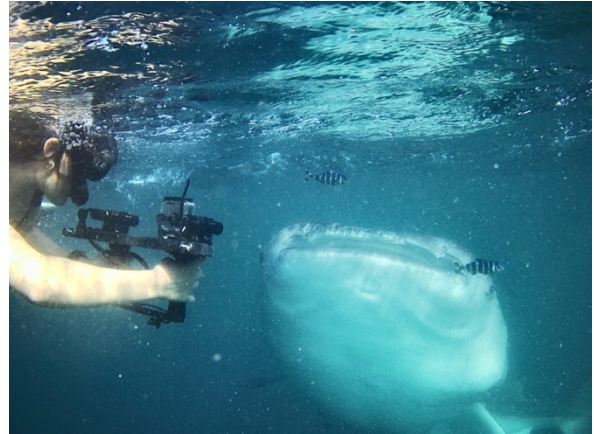


Figure 11. Measurement of the TL of the whale shark with a laser-photogrammetry system.

Source: Sharks Studies Center

While observing the whale shark, several key steps should be followed to ensure accurate data collection and minimize potential sources of error: the survey is turned on and pointed between the tip of the rostrum and the beginning of the first dorsal fin at an appropriate distance and angle from the shark, aligned as parallel as possible to the animal with the green laser points clearly visible on its body.

The most suitable extracted frame is loaded and processed using the digital software Paint as follows: a straight line connecting the two laser points is drawn (line 1), a perpendicular line is traced from the base of the first dorsal fin (line 2), and another straight line is drawn from the tip of the rostrum to the line drawn at point 2. The horizontal pixels are recorded at the two extremities of the line segment for each of the two lines (1 and 3) (Fig. 12).

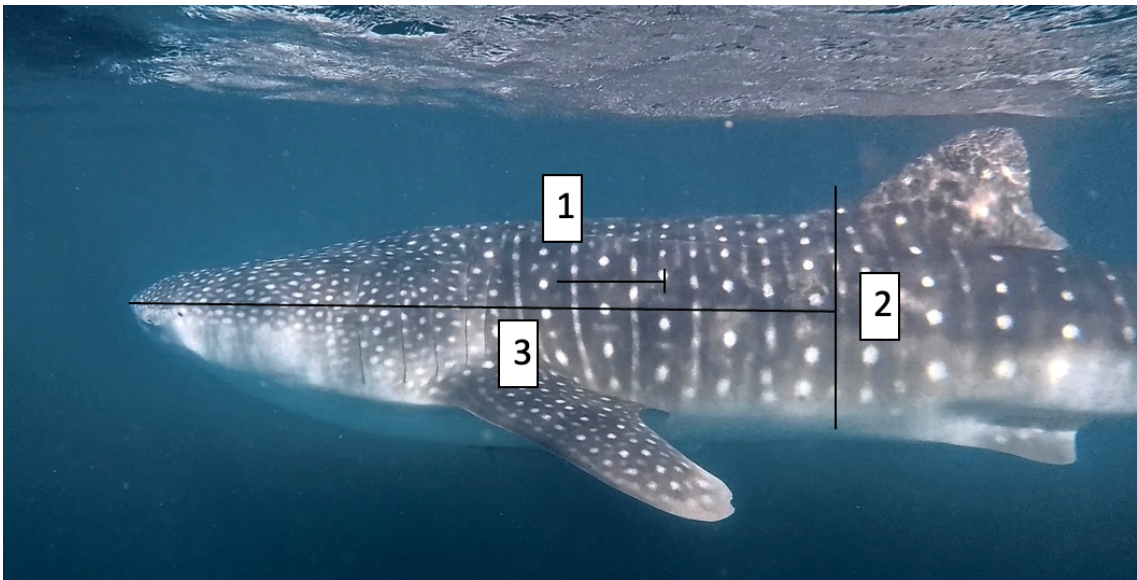


Figure 12. Frame of the whale shark analyzed with Paint. 1) line between the two points of the laser. 2) perpendicular line from the base of the first dorsal fin. 3) line from the tip of the rostrum to the intersection with line 2.

Source: photo by Rebecca Squadroni, Djibouti 2024

The image is then uploaded to an Excel sheet for the second part of the processing.

The pixel reference values taken at the starting and ending points of segments 1 and 3 are respectively subtracted from each other to obtain the total pixels of the two segments. In particular, the numerical value of segment 1 corresponds to 30 cm in pixel value and indicates the distance between the two laser points. The numerical value of segment 3 instead indicates the partial length of the individual being measured.

A proportion is then applied to transform the pixel value of the shark's partial length into centimeters:

$$\text{ref} : \text{obj} = \text{pix ref} : \text{pix obj}$$

$$\text{obj} = (\text{ref} * \text{pix obj}) / \text{pix ref}$$

where: *ref* is the distance between the laser pointers (30 cm), *obj* is the object being measured (the partial length of the shark), *pix ref* and *pix obj* are the respective pixel values measured on the photo of the two segments 1 and 3, respectively.

By doing this, the partial length of the object being measured, which in this case is the specimen of *R. typus*, is calculated. However, only a portion of the shark's length can be obtained using this proportion, specifically the portion corresponding to segment 3 from the tip of the roster to the beginning of the

first dorsal fin. This is because it is very difficult to capture a close-up and complete image of the whale shark due to its size.

Therefore, the calculation of the animal's TL is done using another equation (Matsumoto *et al.*, 2017). First of all, the logarithm of the TL of the animal is calculated:

$$\text{Log TL} = 0.964 * \log \text{obj} + 0.443$$

Then, through the inverse function of the logarithm, the TL of the animal is measured with an average error ranging from 1.4% to 3.3% (Matsumoto *et al.*, 2017).

The final measurement in meters is automatically calculated by Excel, where all the mentioned formulas are imputed along with the pixel measurements of the reference segment and the object segment (Fig. 13).

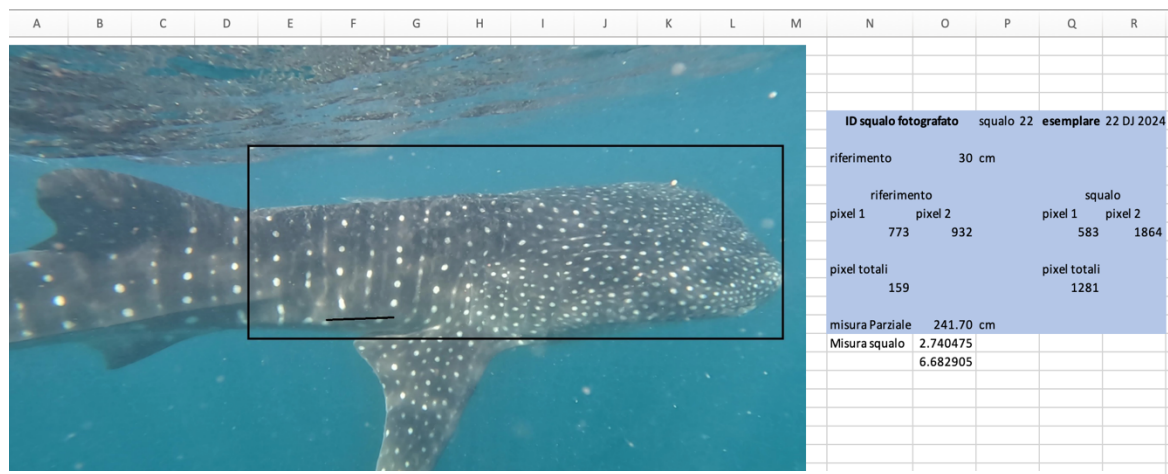


Figure 13. The Excel sheet in which all the equations are automatically imputed to obtain the final measurement that corresponds to the TL of the shark n.22 in Djibouti (2024).

Source: Sharks Studies Center-Scientific Institute

2.5 Surface feeding behaviors

The surface feeding behavior identification was carried out through the systematic recognition and categorization of the three different feeding strategies (passive, active, and vertical) exhibited by *R. typus* during the feeding event.

Initially, each video recording collected during the expedition was observed carefully and only the most representative and detailed videos were taken into consideration. Suitable footage had to provide a clear view of the shark and its activity and encompass a sufficient duration. The starting time of each recording was calculated in seconds (s) from the moment when the mouth and gills of the whale shark were clearly visible. If these features were no longer visible, the stopwatch was paused until they reappeared.

Depending on the density of zooplankton present in the water, shark behaviors were identified following different feeding criteria described by Nelson and Eckert (2007). Based on video analysis, vertical feeding (V) was recorded when the shark was in an almost vertical orientation with its mouth wide open and pointed toward the surface. In this stationary position, the shark feeds by taking significant gulps of water into its mouth, shutting it for a few seconds after each intake, and expelling water through its gill slits.

Passive feeding (P), conversely, was recorded when the shark was swimming forward at a constant speed, moving slowly just below the water's surface. While feeding passively, the shark's mouth is partially closed and the gills slightly opened, without gulping or suctioning observed.

Instead, underwater observations of active feeding (A) showed the shark actively swimming and breaking the surface. This behavior is easily recognizable by the dorsal fin out of the water, mouth wide open like the gills pumping water with frequent head turns and sudden direction changes.

Other non-feeding behaviors, such as 'cruising', were not recorded, as the whale sharks were observed swimming deeper at increased speeds with the mouth and the gills fully closed, moving from one area to another in search of new feeding grounds (Nelson and Eckert, 2007).

Once all surface feeding behaviors were analyzed, they were categorized into an Excel table with their corresponding durations to determine the frequency of the behaviors exhibited by whale sharks.

2.6 Environmental Data Collection

Environmental data provide essential context for studying the feeding ecology, movement patterns, behavior, and habitat preferences of whale sharks. Variables such as SST, ENSO events, chlorophyll-*a* concentration, rainfall, sea

conditions, and wind speed provide insights into the distribution and abundance of planktonic organisms, which are the primary food source for whale sharks. In addition, factors such as SST, upwelling and nutrient-rich zones can predict the migration patterns to feeding grounds and seasonal movements of *R. typus*, providing information for conservation efforts and ecotourism management. Furthermore, as already mentioned, environmental data help to assess the impacts of climate change on whale shark habitat, behavior, and food resources. Environmental data collected during all the scientific expeditions carried out in Djibouti (2017, 2020, 2022, and 2024) and during each trip with zodiacs were:

- A. Sea conditions, obtained from the windguru database (www.windguru.cz) for the Djibouti area and classified as calm, slightly rough, and rough according to the Douglas scale of wave height.
- B. Light levels, expressed in OKTAS, a unit of measurement used to describe the percentage of cloud cover, in terms of how many eighths of sky are covered by clouds, and evaluated by the same operator (Rees, 2001). The measurement intervals used to assess the cloud coverage were:
- 0-2 oktas denoted clear sky.
 - 3-5 oktas denoted partly cloudy sky.
 - 6-8 oktas denoted totally cloudy sky.

- C. Sea surface temperature, or SST, expressed in Celsius degrees ($^{\circ}\text{C}$), collected from the Copernicus database (www.copernicus.eu).
- D. Wind speed, expressed in knots (km/h), collected from the windguru database for the Djibouti area.
- E. Rainfall, measured in millimeters per hour (mm/h), collected from the windguru database for the Djibouti area.
- F. Chlorophyll-*a* concentration, measured in milligrams per cubic meter (mg/m^3), taken from the Copernicus database.
- G. ENSO, expressed in Multivariate Enso Index (MEI), obtained from the NOAA Climate Prediction Center database (www.noaa.gov).
- H. Time of the day, expressed in hours (h) and categorized on the scheduled times of the trips with zodiacs during each day in all the expeditions (scheduled time: 09.00-12.00; or 14.00-17.00).

2.7 Data analysis

The dataset analyzed in this study contains both not directly and not observed factors to deal with endogeneity issues. The former corresponds to seven environmental factors, so labelled: (i) 'okta', denoting light levels; (ii) 'ntemp', describing SST; (iii) 'nrain', denoting weather activity in terms of rainfall; (iv) 'nwspeed', describing wind speed; (v) 'year' referring to the time period; (vi) 'nenso', referring to ENSO measurement unit, evaluated through the MEI; and (vii) 'nchlorop', regarding the concentration of chlorophyll-*a* in mg/m³. Concerning non-directly measured variables, they have been computed as *proxy* discrete variables and consist of two additional environmental factors: (i) 'sea', referring to sea conditions in terms of activity as an ordinal variable, assuming values 1 (whether the sea is calm), 2 (whether the sea is slightly rough), and 3 (whether the sea is rough); and (ii) 'ntime', denoting the time spent during the sightings as *dummy* variable equals to 0 (time slot 09:00-12:00) and 1 (time slot 14:00-17:00). The variable of interest corresponds to 'dbehavior', denoting the whale shark surface feeding behavior. It is computed either as a *dummy* variable equal to 0 (passive) and 1 (active and vertical) to be estimated in the multinomial logistic function or as an ordinal variable equal to 1 (active), 2 (passive), and 3 (vertical) to evaluate any possible outcome in the Best Subset Selection analysis.

The dataset has been further arranged to better analyze the degree of interdependence and/or relationship between non-directly and non-observed factors. More precisely, some variables have been grouped into classes and then evaluated as categorical or ordinal discrete indicators. They are: SST, assuming values 0 for the class ≤ 26 °C and 1 for the class > 26 °C; rainfall, assuming values 0 for the class 0.0 mm/h and 1 for the class > 0.0 mm/h; wind speed, taking values 1 for the class 3.0–6.9 knots, 2 for the class 7.0–9.9 knots, and 3 for the class 10.0-12.9 knots; MEI, assuming values 0 for the class between -0.9 and 0.0, and 1 for the class between 0.1 and 2.0; and presence of chlorophyll-*a*, taking values 1 for the class 0.00-0.50 mg/m³, 2 for the class 0.51-2.00 mg/m³, and 3 for the class ≥ 2.01 mg/m³. Every group of classes has been computed based on its median on the sample size (1082 surface feeding behaviors recorded), so that each class is equally distributed and weighted when making inferences.

First of all, a correlation matrix has been performed to deal with potential (multi)collinearity problems that let the predictors be strongly correlated between them (referring to similar events).

In the second step, a multinomial logistic regression function is evaluated to study in detail the relationship between the feeding behaviors and the predictors affecting them. Here, we recall that the variable of interest denoting the whale

shark surface feeding behavior has been computed as a categorical variable: = 1 active/vertical and = 0 passive. The connection between active and vertical behavior is because the latter would mean that the whale shark is inclined to assume a sort of active predation behavior (Di Capua *et al.*, 2021). The (multinomial) logistic function is:

$$(1) y_i = \sum_{j=1}^k X_{ki} \gamma_k + \varepsilon_i$$

where $n = 1,082$, X_{ki} refers to the matrix containing all seven predictors evaluated in the first step, γ_k are the regression parameters to be estimated, and ε_i denotes the error term (or causal component).

Finally, in the third step, before computing and comparing (sample) marginal effects for every predictor across units over time, a discriminant analysis is performed. This latter focuses on selecting the ‘best’ submodel solution (or covariates) affecting the outcomes of interest and avoid potential (multi)collinearity problems among strictly correlated predictors.

The estimating procedure takes the name of Best Subset Selection (BSS) analysis and consists of building and, in turn, comparing several possible regression models based upon an identified set of covariates. The ‘best’ submodel solution, where ‘best’ stands for the subset of predictors better fitting

the data, corresponds to the one with the lowest Bayesian Information Criterion (BIC). The BSS and the logit regression are classified as Machine Learning (ML) algorithms. Let the logit model estimate in equation (1), the (sample) marginal effects are computed as:

$$(2) \quad \frac{\partial F(X_{ki}\gamma)}{\partial x_{ki}} = f(X_{ki}\gamma) * \gamma_k$$

where x_{ki} denotes each predictor accounted for.

In this context, let strong correlation matter among covariates, Odds Ratios (OR) have been computed for each predictor, evaluating the probability of an event favorable to an outcome. They correspond to the exponential of the estimated regression parameters $\hat{\gamma}_k$ and their related probabilities are computed as $(1 - OR) * 100$. The usefulness of using OR in terms of probability is because of: (i) strong correlation between predictors underestimating the (sample) marginal effects; (ii) multivariate classification based on discrete variables; and (iii) property of the probabilities assuming values 0 up to 1, according to the possibility to reach infinite values in case of (multi)collinearity problems.

In this study, confusion matrix is applied to multiclass classification problems based on the estimates achieved in the BSS analysis. An advantage of the

confusion matrix is the ability to compute the predictive capability to verify the accuracy (or consistency) of the estimates achieved in a ML classification algorithm. In this section, we consider the variable of interest built as ordinal factor to understand how sea/climatic factors affect every possible surface feeding behavior and why whale sharks are inclined to assume active (A), passive (P), or vertical (V) actions. Every confusion matrix has been interpreted in terms of probability to better evaluate the results. The elements inside the table denote the joint probabilities. The predictive capability is computed as: $1 - \text{mean}(\%)$, where the mean is obtained by the ratio between the outcomes on the main diagonal (representing the number of successes and failures) and the total observations.

In addition, a Cochran's Q test is conducted to emphasize the strong dependency between whale shark feeding behavior and all the other variables, examining independence (or causal choice, under the null hypothesis) and dependence (or not causal choice, under the alternative hypothesis) between these variables.

The last insight is addressed by means of a Chi-square test of independence to investigate whether ENSO measurement unit (MEI) and sightings over time are dependent (alternative hypothesis) or independent (null hypothesis) between them.

More precisely, the hypothesis testing assumes that the two variables ('year' and 'nenso') are likely to be not related (independency under the null) or related (dependency under the alternative). The test statistic is computed as:

$$(3) \chi^2 = \frac{\sum_i \sum_j (n_{(i,l)} - \hat{n}_{(i,l)})^2}{\hat{n}_{(i,l)}}$$

where $n_{(i,l)}$ denote the absolute joint frequency, where i and l are numerical indices referring to two discrete variables and $\hat{n}_{(i,l)}$ stands for the absolute joint frequency in case of independence.

However, since the data have been collected on four non-consecutive years only, a related confusion matrix is computed to analyze in depth that result.

3. Results

3.1 Photoidentification

A total of 81 individuals have been identified in the database of the Sharks Studies Center-Scientific Institute using the pattern recognition software I³S *Classic* from 2017 to 2024. More precisely, in January 2017 and 2020, 5 and 6 sharks were identified, respectively, in January and November 2022, 27 and 10 sharks were identified, respectively, and in January 2024, 33 new individuals were added to the database. Specifically, in January 2024, 15 resightings occurred. Among these, 2 individuals were resighted from 2020, and 13 from 2022.

All the individuals observed were males, identified by filming the presence of two claspers in the pelvic area.

3.2 Laser-photogrammetric survey

A laser-photogrammetric survey was conducted on 18 out of the 48 whale sharks (33 new individuals and 15 resightings) observed during the expedition carried out in January 2024. Among these, 10 were identified as new individuals in 2024, while 8 sharks were previously sighted in earlier

expeditions, including 1 shark from the 2020 expedition and 7 sharks from the 2022 expedition. The total length (TL) of every measured whale shark is reported in Figure 14, with an average value of 6.4 ± 0.1 m for all 18 individuals. According to the results, the largest individuals were the numbers 13A and 15A, with a TL of 7.1 ± 0.1 m and the smallest one was the number 23B, with a TL of 5.6 ± 0.1 . Additionally, two sharks were measured both in 2022 and 2024, allowing size growth evaluation. The size of shark number 1B in 2022 was 6.36 m and 6.5 m in 2024, indicating a growth of 0.14 m; whereas shark number 15B, whose size in 2024 was 6.1 m, appears to have grown by 0.26 m compared to 2022, where the TL was 5.84 m.

Analysis of TLs revealed that all measured whale sharks were immature. Indeed, several authors suggested that male whale sharks generally attain sexual maturity at around 8 meters in TL, based on clasper morphology (Graham and Roberts, 2007; Norman and Stevens, 2007; Hsu *et al.*, 2014; Meekan *et al.*, 2020; Pierce *et al.*, 2021).

Laser-photogrammetric survey

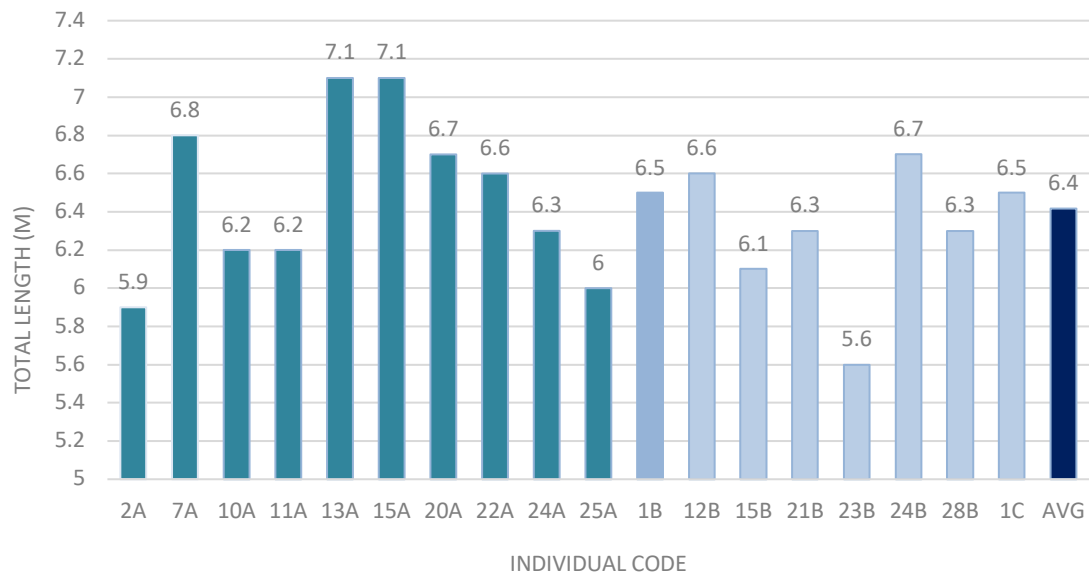


Figure 14. Laser-photogrammetric measurements of 18 sharks. The individuals n. 2A, 7A, 10A, 11A, 13A, 15A, 20A, 22A, 24A, and 25A are new recorded individuals from the 2024 expedition (darker in color columns). The individuals n.1B, 12B, 15B, 21B, 23B, 24B, 28B and 1C are resightings from 2022 and 2020 expeditions respectively (lighter in color columns). The last column on the right shows the average TL of all the measured whale sharks (darkest in the color column).

3.3 Surface feeding behaviors

The exhibited surface feeding behaviors were examined and categorized with their respective durations (s) to determine the frequency (%) of each behavior among whale sharks. Based on the results shown in Table 1, the most observed whale shark filter feeding strategy was vertical feeding (V) (53.69%), followed by active feeding (A) (27.51%), and passive feeding (P) (18.80%).

Table 1. Total time of different surface feeding behaviors exhibited by the whale sharks in seconds (s) and frequencies (%) in the 2024 expedition in Djibouti. (A) stands for active; (P) for passive; and (V) for vertical feeding behaviors.

Feeding behavior	Time (s)	Time (%)
A	6678	27.51%
P	4563	18.80%
V	13034	53.69%
Total	24275	100%

Previous expeditions (2017, 2020, and 2022) of the Sharks Studies Center showed different results regarding the frequencies of surface feeding behaviors exhibited by whale sharks compared to 2024 (Table 2). Specifically, in 2017, the most observed surface feeding behavior was passive (54.91%), similar to January 2022 (44.56%), whereas in 2020, vertical feeding predominated (56.67%), mirroring November 2022 (49.49%).

Table 2. Frequencies (%) of the whale shark surface feeding behaviors for each expedition (January 2017, January 2020, January 2022, November 2022, and January 2024) in Djibouti. (A) stands for active; (P) for passive; and (V) for vertical feeding behaviors.

Feeding behavior	Jan 2017	Jan 2020	Jan 2022	Nov 2022	Jan 2024
A	14.01%	23.21%	19.88%	24.62%	27.51%
P	54.91%	20.12%	44.56%	25.89%	18.80%
V	31.08%	56.67%	35.56%	49.49%	53.69%
Total	100%	100%	100%	100%	100%

3.4 Statistical analysis of the feeding behavior of whale sharks

3.4.1 Correlation matrix

Regarding the correlation matrix (Tab. 3), the variables resulting strongly correlated with more than one predictor were ‘nenso’ (with ‘ntemp’, ‘nwspeed’, and ‘nrain’ displaying a correlation function $\geq 55\%$), and ‘year’ (with ‘sea’, ‘nenso’, and ‘nwspeed’ displaying a correlation function $\geq 40\%$). Thus, these two variables were dropped, considering 7 out of 9 variables overall.

	year	okta	sea	ntemp	nwspeed	nrain	nenso	nchlorop
year	1	-0.679	0.852	0.747	-0.666	-0.369	0.789	-0.259
okta	-0.679	1	0.247	-0.594	0.377	0.230	-0.794	0.055
sea	0.010	0.247	1	0.057	0.738	0.022	-0.061	0.121
ntemp	0.747	-0.594	0.057	1	-0.192	-0.172	0.891	-0.367
nwspeed	-0.266	0.377	0.738	-0.192	1	0.176	-0.344	0.287
nrain	-0.369	0.230	0.022	-0.172	0.176	1	-0.096	-0.029
nenso	0.789	-0.794	-0.061	0.891	-0.744	-0.696	1	-0.422
nchlorop	-0.259	0.055	0.121	-0.367	0.287	-0.029	-0.422	1

Table 3. Correlation matrix between the predictors

3.4.2 Multinomial Logistic Regression Model

All predictors were significant at least at 1% (Tab. 4), highlighting the efficiency of the supervised ML algorithm in minimizing the sum of squared residuals and addressing the potential (multi)collinearity. Indeed, the full (or unrestricted) model, with all nine predictors, showed an Akaike Information

Criterion (AIC) of 333.40, while the restricted model (without 'nenso' and 'year') had an AIC of 311.89. The lowest AIC was the most preferred (restricted model).

Looking at the table 4, the values 'okta', 'sea', 'nrain', and 'nclorop' had a positive z-value, while 'ntemp', 'nwspeed', and 'ntime' had a negative z-value, indicating a significant effect of predictors on whale shark surface feeding behavior. By construction, higher values of 'sea' refer to worse sea conditions. Specifically, factors such as lower light intensity, cloudier sea, rainfall, and higher chlorophyll-a levels affected positively the whale shark feeding behavior towards A/V strategies ($y=1$). On the contrary, higher SST, strong wind speed, and afternoon hours affected negatively the whale shark feeding behavior towards P strategy ($y=0$).

Coefficients	Estimate	SE	z-value	Pr(> z)
okta	3.051	0.038	80.29	0.00***
sea	3.033	0.128	23.70	0.00***
ntemp	-2.023	0.135	-14.99	0.00***
nwspeed	-1.302	0.141	-9.23	0.00***
nrain	3.438	0.145	23.71	0.00***
ntime	-1.652	0.141	-11.72	0.00***
nclorop	2.405	0.201	11.97	0.00***

Table 4. Multinomial logistic regression functions analyzing how sea/climatic factors affect whale shark surface feeding behavior across units over time. Here, ‘Coefficients’ refers to the covariates; ‘Estimate’ refers to $\hat{\gamma}_k$ (the estimated regression parameters γ_k); ‘SE’ stands for Standard Error; ‘z-value’ denotes the test statistic obtained for each predictor (the ratio between ‘Estimate’ and ‘SE’); and ‘Pr(>|z|)’ refers to the associated p-value according to a two-sided hypothesis testing (where the null stands for non-significance). The significance levels are: (*) significance at 10%; (**) significance at 5%; and (***) significance at 1%.

The predictor ‘nrain’ should be interpreted with care. The maximum mm/h collected during the sightings has been 0.1 and it should be interpreted as: less rainfall is observed with A (and/or V) feeding behavior.

3.4.3 Best Subset Selection (BSS)

A BSS has been performed to better evaluate (and then confirm) the results achieved in the multinomial logistic regression. According to Figure 15, the ‘best’ subset of predictors corresponded to the ones with lower BIC (positive

values). More precisely, the best subsets inclining the whale sharks to assume A (or V) feeding behavior were associated with values of SST ≤ 26.2 °C, chlorophyll-*a* ≥ 0.60 mg/m³ (assuming values 2 and 3 by construction), rainfall ≤ 0.1 mm/h, and ENSO measurement unit lined up on ≤ -2.1 . The ‘nchlorop’ with value 0.473 mg/m³, even if displaying more black squares than the values of ≥ 0.60 mg/m³, has been discarded from the discriminant analysis because of its significance at a highly larger BIC as well (from 23 to 51).

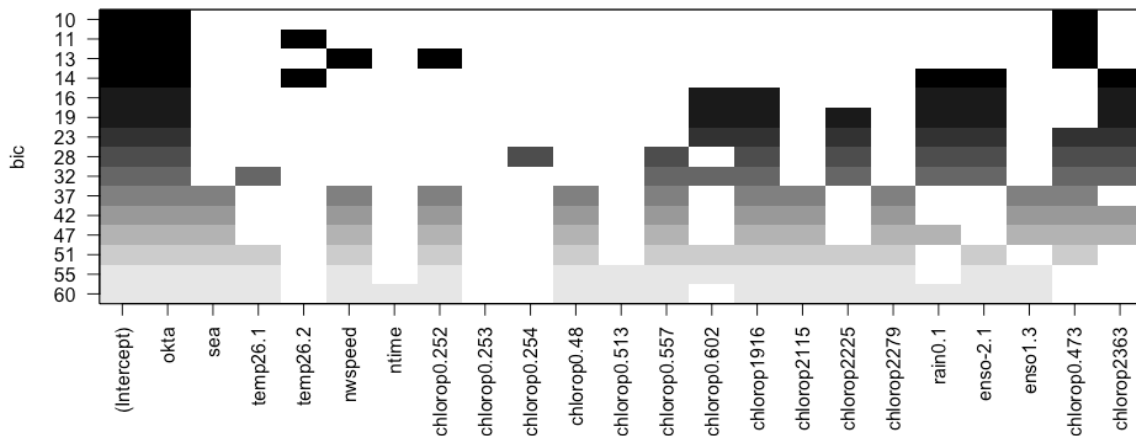


Figure 15. Best Subset Selection shrinking procedure is assessed on the dataset accounting for all possible outcomes of each predictor. Here, ‘temp’ stands for SST; ‘rain’ denotes rainfall; ‘chrolop’ refers to the number of chlorophyll-*a*; and ‘enso’ stands for ENSO measurement unit. The black squares refer to stronger effect of every predictor on the outcomes of interest ($y=1$), corresponding to the lowest BIC (positive values).

3.4.4 Odds Ratio and Sample Marginal Effects

According to the estimates displayed in Table 5, the main factors affecting whale shark surface feeding behavior, in order of importance, were ‘nchlorop’

(79.80%), ‘okta’ (64.15%), ‘nrain’ (62.50%), ‘ntemp’ (59.26%), ‘sea’ (49.66%), ‘nwspeed’ (44.24%), and ‘ntime’ (26.59%). Finally, a White’s heteroskedasticity correction test has been performed to standardize the residuals dealing with potential (multi)collinearity problems.

Table 5. Sample marginal effects for each observation unit, given n observations, are accounted for. Here, ‘Coefficients’ refers to the factors within the model; ‘dF/dx’ denotes the partial derivatives displaying the marginal effects of the predictors (x'_{ik}) on y_i (‘dbehaviour’); ‘SE’ stands for Standard Error; ‘z-value’ denotes the test statistic obtained for each predictor; and ‘Pr(>|z|)’ refers to the associated p-value in a two-sided hypothesis test (where the null accounts for non-significance). The significance levels are: (*) significance at 10%; (**) significance at 5%; and (***) significance at 1%.

Coefficients	dF/dx	SE	z-value	Pr(> z)
okta	0.430	0.143	3.01	0.00***
sea	0.286	0.127	2.25	0.01**
ntemp	-0.415	0.172	-2.41	0.01**
nwspeed	-0.276	0.131	-2.11	0.02**
nrain	0.367	0.176	2.09	0.02**
ntime	-0.201	0.115	-1.75	0.04**
nchlorop	0.413	0.141	2.93	0.00***

3.4.5 Confusion Matrices

A confusion matrix was then used for each of the main factors affecting whale shark surface feeding behavior: ‘nchlorop’, ‘okta’, ‘rain’, and ‘temp’. The last three predictors (‘sea’, ‘nwspeed’, and ‘ntime’) have been evaluated through

ENSO measurement unit, discarded from the analysis because of their strong correlation. In this context, SST and MEI are not considered to be grouped into classes to investigate their possible value.

The first confusion matrix (Tab. 6) highlighted that either A or V feeding behavior had the highest probabilities when ‘nchlorop’ assumed value 2 (between 0.51-2.00 mg/m³ by construction). Conversely, P feeding behavior had the highest probability when ‘nchlorop’ assumed values 1 or 3.

The predictive capability was 83.20%.

Table 6. Confusion matrix between behavior and chlorophyll-*a*. The values inside the table correspond to the joint probabilities between two discrete variables (Y and X) for each possible outcome. Here, Y refers to whale shark surface feeding behavior: (A) active surface ram-feeding, (P) ram (or passive)-feeding, (V) vertical feeding, and X refers to the number of chlorophyll-*a* grouped in classes. The sum of each row denoting the variable of interest gives one referring to probabilities.

behavior/chlorophyll-<i>a</i>	1	2	3
1 (A)	0.187	0.614	0.199
2 (P)	0.703	0.123	0.174
3 (V)	0.223	0.637	0.140

According to light levels and whale shark surface feeding behavior in the second confusion matrix (Tab. 7), when the okta measurement unit increased up to the maximum value (=8), A and V feeding behaviors increased, exceeding

the P feeding strategy. Conversely, better light levels (low okta) corresponded to P feeding behavior. The predictive capability was 84.46%.

Table 7. Confusion matrix between behavior and okta. The values inside the table correspond to the joint probabilities between two discrete variables (Y and X) for each possible outcome. Here, Y refers to whale shark behavior: (A) active surface ram-feeding, (P) ram (or passive)-feeding, (V) vertical feeding, and X refers to light levels measured through the predictor ‘okta’. The sum of each row denoting the variable of interest gives one referring to probabilities.

behavior/okta	0	1	2	3	4	5	6	7	8
(A)	0.014	0.017	0.021	0.032	0.439	0.055	0.073	0.106	0.261
(P)	0.102	0.120	0.101	0.068	0.505	0.035	0.021	0.062	0.107
(V)	0.010	0.012	0.048	0.024	0.445	0.050	0.062	0.136	0.225

In Table 8, the third confusion matrix between whale shark feeding behavior and rainfall was displayed. The total absence of rain was associated with P strategy (value 0), while more rainfall corresponded to A and V strategies (value 1). The accuracy lined up at 88.80%.

Table 8. Confusion matrix between behavior and rainfall. The values inside the table correspond to the joint probabilities between two discrete variables (Y and X) for each possible outcome. Here, Y refers to whale shark behavior: (A) active surface ram-feeding, (P) ram (or passive)-feeding, (V) vertical feeding, and X refers to rainfall. The sum of each row denoting the variable of interest gives one referring to probabilities.

behavior/rainfall	0	1
(A)	0.005	0.996
(P)	0.069	0.931
(V)	0.035	0.965

Concerning the fourth confusion matrix regarding the SST (Tab. 9), the optimal value was > 26 °C. Thus, the SST values used were 26.1 and 26.2 °C, just as found in BSS analysis, and 28.07 as mean of the °C in 2024. The A feeding behavior corresponded to medium SST (26.2 °C), while higher SST (28.07 °C) was associated with P and V feeding behaviors. Lower SST (26.1°C), instead, was associated with P feeding strategy. The predictive accuracy was 88%.

Table 9. Confusion matrix between behavior and SST. The values inside the table correspond to the joint probabilities between two discrete variables (Y and X) for each possible outcome. Here, Y refers to whale shark behavior: (A) active surface ram-feeding, (P) ram (or passive)-feeding, (V) vertical feeding, and X refers to SST. The sum of each row denoting the variable of interest gives one referring to probabilities.

behavior/SST	26.1	26.2	28.07
1 (A)	0.012	0.894	0.094
2 (P)	0.058	0.069	0.873
3 (V)	0.039	0.143	0.818

Finally, last confusion matrix between whale shark surface feeding behavior and MEI was evaluated (Tab. 10). Values equal to ≤ -2.1 corresponded to A feeding strategy (as found in BSS analysis). Conversely, an increase in MEI was associated with V and, in less quantity, P feeding behaviors. The predictive capability lined up at 88.4%.

Table 10. Confusion matrix between behavior and MEI. The values inside the table correspond to the joint probabilities between two discrete variables (Y and X) for each possible outcome. Here, Y refers to whale shark behavior: (A) active surface ram-feeding, (P) ram (or passive)-feeding, (V) vertical feeding, and X refers to ENSO measurement unit measured through MEI. The sum of each row denoting the variable of interest gives one referring to probabilities.

behavior/MEI	-2.1	-0.3	2.0
1 (A)	0.811	0.075	0.116
2 (P)	0.072	0.009	0.920
3 (V)	0.053	0.029	0.926

The Cochran's Q test statistic was equal to -211.80, supporting the dependence between variables and rejecting the null hypothesis (p-value close to zero). The significance level was 5% as the default, with one degree of freedom.

3.4.6 ENSO and interannual sightings of the whale sharks

Regarding the Chi-square test of independence, let the test statistic be 250, with p-value close to zero, and 3 degrees of freedom, we can reject the null in favor of the alternative hypothesis. However, since the data have been collected on four non-consecutive years only, a related confusion matrix was computed to analyze in depth that result. According to Table 11, with predictive capability equal to 88%, the highest number of sightings has been recorded in 2024 (832

sightings), with a MEI around 2 enouncing El Niño event, followed by lower sightings as MEI decreases progressively to La Niña events (in 2020 with MEI -2.1, and in 2017 and 2022 with $MEI \cong -0.20$).

Table 11. Confusion matrix between yearly sightings and MEI. The values inside the table correspond to the joint probabilities between two discrete variables (Y and X) for each possible outcome. Here, Y refers to total sightings per year and X refers to ENSO measurement unit measured through MEI. The sum of each row denoting the variable of interest gives one referring to probabilities.

year/MEI	-2.1	-0.2	2.0
2017	0.000	1.000	0.000
2020	1.000	0.000	0.000
2022	0.000	1.000	0.000
2024	0.000	0.000	1.000

4. Discussion

4.1 Photoidentification

The January 2024 expedition in Djibouti has led to the addition of 33 new observed and identified whale sharks in the database, making a significant contribution for the ecology and ethology of this species. Additionally, researchers recorded numerous resightings of the same shark, observed at different times within the same day or on different days.

The non-invasive approach through photoidentification tools allowed researchers to distinguish between new individuals and resightings using the I³S *Classic* software, confirming that both whale shark flanks above the pectoral fins, just posterior to the gill slits, had unique patterns that remained unchanged over time (Colman, 1997; Arzoumanian *et al.*, 2005; Brooks *et al.*, 2010).

Overall, the identification of 81 whale sharks from 2017 to 2024 confirms that Djibouti hosts an important population. This finding is consistent with previous studies carried out in the same area by Boldrocchi *et al.* (2020), who photo-identified 190 whale sharks between 2015 and 2018, and Rowat *et al.* (2011), who reported 297 individuals identified between 2003 and 2010.

However, in January 2024, the highest percentage of sightings (33) compared to the previous years was observed. This increase in sightings over the years

can be primarily attributed to the substantial rise in zooplankton biomass recorded during the years. For instance, zooplankton biomass in the Gulf of Tadjoura increased from $24.8 \pm 9.1 \text{ mg/m}^3$ in 2017 (Di Capua *et al.*, 2021) to $42.2 \pm 31.9 \text{ mg/m}^3$ in 2018 (Boldrocchi *et al.*, 2020). However, the annual concentration of zooplankton biomass was not provided in this study. Nonetheless, Copernicus satellite-data for the study area showed a constant increase of concentration in chlorophyll-*a* in 2020 (0.47 mg/m^3), 2022 (0.53 mg/m^3), and 2024 (0.61 mg/m^3) compared to 2017 (0.25 mg/m^3), which may have enhanced the zooplankton abundance and in turn determined an increase in the number of whale sharks sightings over time.

Zooplankton is the primary food source for whale sharks, and its abundance plays a critical role in determining their distribution and aggregation patterns across different tropical regions (Bava *et al.*, 2022), including Mexico (Motta *et al.*, 2010; Hoffmayer *et al.*, 2007), Tanzania (Rohner *et al.*, 2015), Indonesia (Marliana *et al.*, 2018), and Djibouti (Boldrocchi *et al.*, 2020; Di Capua *et al.*, 2021). Boldrocchi *et al.* (2020) showed a correlation between zooplankton biomass variation and whale shark distribution, highlighting that the increased zooplankton biomass in Djibouti may be a key factor driving the gathering of whale sharks off the coast.

In 2024, 15 identified whale sharks were resighted at least once from the previous years of 2020 (2 specimens) and 2022 (13 specimens), revealing that some individuals could have prolonged residency in Djibouti (Boldrocchi *et al.*, 2020). While the movements of whale sharks during aggregation periods are well documented, their long-distance movements outside the off seasons remain unclear. Satellite tagging revealed that few individuals from Djibouti have moved into the Red Sea and northern Indian Ocean (Rowat *et al.*, 2016), and some Red Sea whale sharks reached the Gulf of Aden, without going in the Gulf of Tadjoura (Berumen *et al.*, 2014). Additionally, recent research suggests movements from the Red Sea to the Gulf of Aden, without approaching Djibouti (Cochran *et al.*, 2019). It is difficult to determine whether these movements represent migration between aggregation sites of year-round residence in Djibouti. Further satellite tagging should confirm if this seasonal migration path for Djibouti whale sharks could be related to the movement in search of better feeding opportunities or if there is site-fidelity in at least some whale sharks' individuals.

In 2024, as well as in the previous years, all newly identified individuals were juvenile males, exhibiting short and smooth claspers. This is in line with previous studies (Rowat *et al.*, 2011; Boldrocchi *et al.*, 2020), confirming that Djibouti is a male sex-based aggregation, as well as other aggregation sites

across the Indian Ocean. For instance, the population structure of whale sharks observed in Mozambique (74%) and Tanzania (89%) was mostly male-dominated, with the majority being immature (Rohner *et al.*, 2015). Similarly, in the Philippines, 96.5% of the 183 identified individuals were immature males (Araujo *et al.*, 2019), while in the Seychelles males comprised 82% of the observed population.

Segregation is common in many shark species, including whale sharks, which exhibit significant sex- and size-based segregation (Rohner *et al.*, 2015). This appears to be driven by differing nutritional needs, swimming abilities or to minimize intra-specific competition, aggression, and predation (Wearmouth and Sims, 2008). Despite evidence of potentially varying diet preferences between juveniles and adults (Boldrocchi *et al.*, 2020; Rohner *et al.*, 2015), the prevalence of juvenile male whale sharks at known aggregation areas is still under investigation.

In Djibouti, the prevalence of immature males and the low presence of both mature and immature females, as well as mature males, suggest that mating may not be the primary reason of the whale sharks' aggregation in these sites. Instead, they are more likely to gather for feeding purposes. While male-dominated aggregations of whale sharks are more commonly observed, there are indeed locations where female-dominated aggregations have been

documented, like in the Galapagos Island, with a great majority (91.5%) of pregnant females (Acuña-Marrero *et al.*, 2014) or in the Gulf of California, where adult females migrate regularly from year to year (Ramírez-Macías *et al.*, 2012). In addition, juvenile sharks tend to favor coastal, shallow waters for foraging, while larger adult sharks are commonly found in open ocean environments or areas with high productivity, such as underwater seamounts and continental shelves (Rowat and Brooks, 2012; Ramírez-Macías, 2017).

4.2 Laser-photogrammetric survey

Analysis of data processed using laser-photogrammetry in 2024 revealed that the average TL of whale sharks in Djibouti was 6.4 m, similar to the one obtained in January and November 2022 of 6.14 m and 6.05 m respectively, confirming that Djibouti area is frequented annually during the season by immature individuals (Boldrocchi *et al.*, 2020). This suggests that immature whale sharks gather in the coast of Djibouti to exploit an abundance of food, which is likely the result of environmental changes such as ocean temperature fluctuation and currents, to maintain their fast growth rates (Meekan *et al.* 2015).

It is known that whale sharks have an estimated longevity of about 80 years (Fishbase, <http://www.fishbase.org>). Despite no studies are available about the

growth rate of whale sharks in Djibouti, in Ningaloo Reef male and female growth profiles differ. Males exhibit a slightly faster growth rate in the first decade but slowing as they approach asymptotic growth in the latter stages of the lifespan. Conversely, females display lower initial growth rates that are more sustained throughout their lifespan, resulting in a more indeterminate growth pattern with larger size-at age past approximately 20 years (Meekan *et al.*, 2020).

Results from this study reflect the trend of faster growth in juvenile males, with an increase in TL of about 0.20 m measured over just two years apart (from 2022 to 2024).

4.3 Influence of environmental factors on feeding behaviors

Environmental changes significantly influenced the different surface feeding behaviors exhibited by whale sharks over different years. The main drivers of the whale shark choice were, in decreasing order, chlorophyll-*a* concentration, oktas, rainfall, surface water temperature, sea conditions, wind speed, and time of the day.

Chlorophyll-*a* concentration is a proxy of phytoplankton biomass (Sequeira, 2012), which in turn affects zooplankton availability (Rohner, 2017). Several studies have demonstrated the positive correlation between chlorophyll-*a*

concentration and zooplankton abundance (Hacohen-Domené *et al.*, 2015; Ranintyari *et al.*, 2018; Boldrocchi *et al.*, 2020; Manuhutu *et al.*, 2021).

In the current study, areas with higher chlorophyll-*a* concentrations (≥ 0.60 mg/m³) are likely to support higher zooplankton biomass available as prey for whale sharks, which have been shown to use A and V feeding strategies. On the contrary, in good sea and weather conditions, together with lower (≤ 0.60 mg/m³) or massive presence of chlorophyll-*a* (≥ 2.01 mg/m³), whale sharks exhibit a shift in their feeding behavior from A or V to P feeding, because it would require less effort while searching for higher density of food (Rohner & Prebble, 2021).

In 2017, the preference of P feeding strategy can be explained by favorable sea and weather conditions of the year. During such conditions, the concentration of chlorophyll-*a* tends to decrease, leading to lower prey availability. Indeed, Di Capua *et al.* (2021) also recorded the lowest abundance of zooplankton during 2017, justifying the inclination of the whale shark to adopt a P feeding behavior. In fact, actively searching for prey would have outweighed the energy benefits, whereas P feeding allowed the sharks to optimize their efforts for maximum output.

On the contrary, the year 2020 was characterized by generally worse sea and weather conditions which triggered an increase in chlorophyll-*a* concentration

and, consequently, zooplankton biomass. All these environmental variables supported the tendency of whale sharks to choose V feeding strategy.

In January 2022, higher okta levels were recorded, with P feeding being the most observed strategy. This scenario would typically predict A and V feeding strategies, instead of P one. However, other factors like chlorophyll-*a* levels and the absence of rainfall may justify the choice of P feeding strategy. Instead, in November 2022, V feeding was the preferred behavior of the whale sharks with higher light levels and higher chlorophyll-*a* concentrations, as well as in 2024.

Similarly, basking sharks (*Cetorhinus maximus*) adjust their feeding strategies in response to environmental predictors such as chlorophyll-*a* concentration and abundance of prey (Finucci, 2021). According to Sims and Quayle (1998), when zooplankton abundance is below 1g/m^3 , basking sharks exhibit a passive strategy. Conversely, in patches with higher zooplankton density (from 1 to 3g/m^3), they actively forage for plankton to make the effort worthwhile.

Given that chlorophyll-*a* was the most important environmental factor influencing the feeding choice, it is important to understand how its concentration was regulated and affected by all the other environmental factors. Generally worse climate conditions are associated with whale sharks feeding actively or vertically, mostly because the concentration of chlorophyll-*a* tends

to increase with cloudier conditions (higher okta values), less underwater visibility and higher rainfall.

The whale shark is known to not rely on visual acuity when locating and capturing prey, but rather on hearing and olfactory senses (Dove, 2015). Therefore, the whale shark surface feeding behavior in Djibouti is probably influenced by light levels only if associated with rainfall and increasing chlorophyll-*a* events, given their positive correlation.

Regarding SST, chlorophyll-*a* is inversely correlated to SST, which means that as the SST raise, the chlorophyll-*a* decrease. During autumn, the northeast monsoon enables an increase in chlorophyll-*a* that coincides with colder SST and induces an upwelling event along the southern coastline of the gulf of Somalia, causing a nutrient enrichment (Gittings *et al.*, 2016). Upwelled cold waters converge with the warm waters of the Red Sea, creating ideal conditions for the proliferation of phytoplankton and, consequently, zooplankton biomass along the coastline of Djibouti (Boldrocchi *et al.*, 2019). As a result, whale sharks in Djibouti can find rich feeding grounds, actively filtering water to consume vast quantities of prey. However, as SST rises, whale sharks switch to V or P feeding behaviors, which are more energy-efficient in these environmental conditions.

According to Sequeira *et al.* (2013), predicted rises in SST would increase metabolic rates of ectotherm animals, like the whale shark, thereby leading to increased food demands and potentially altering their feeding strategies as prey availability shifts. Indeed, Hachoen-Domené (2015) found that presence of whale sharks in Cabo Catoche and Isla Contoy (Mexico) may be driven by an increase in temperature triggering the spawning of little tuna, given that these areas are characterized by lower primary and secondary production. It does not seem to be the case of whale sharks in Djibouti, since they feed mainly on high concentrations of zooplanktonic prey (Boldrocchi *et al.*, 2018, 2020; Di Capua *et al.*, 2021). However, seven whale sharks in Djibouti have also been observed feeding on a school of anchovies when dense patches of zooplankton were not available (Boldrocchi and Bettinetti, 2019).

Another variable that negatively affects chlorophyll-*a* is the wind speed, meaning that with stronger winds whale sharks tend to do P feeding strategy. According to Rowat *et al.* (2009) and Sleeman *et al.* (2010), higher wind speeds negatively affected both the number of sharks recorded in the Seychelles and Australia, respectively, and caused surface disturbance and prompting a change in shark behavior. It is possible that in Djibouti stronger winds dispersed dense zooplankton patches (Gittings *et al.*, 2016), inducing the whale shark to switch from A/V to P strategy just below the surface. This suggests that during

afternoon hours, when wind speeds are higher, whale sharks would favor a P feeding behavior. Conversely, during lower wind intensity, which often occurs in the morning, zooplankton patches are less dispersed, allowing whale sharks to engage in A and V feeding.

Since worse sea conditions are a consequence of stronger wind speeds, whale sharks may adopt a P feeding strategy with rough sea. However, our results suggested that worse sea conditions increased the concentration of chlorophyll-*a*, and slightly rough sea drove sharks to do A or V feeding behaviors, while P feeding strategy was adopted with calm sea. Since both sea conditions and wind speed were of less importance in influencing the surface feeding behavior, it is possible that other factors, such as currents, can drive the choice of the feeding behaviors. However, this environmental parameter has not been considered in our research and further studies are required to investigate its effectiveness on whale sharks feeding strategies.

The time of the day was the last environmental factor to influence the choice of the filter-feeding strategy. During the morning whale sharks tended to exhibit A or V feeding behavior, probably because dense patches of prey were more available during this time, while during the afternoon they preferred P strategy. Since diel patterns in surface feeding activity in Djibouti have never been described, it is difficult to assess if the distribution of prey in this area

underwent horizontal and/or vertical diel changes. Decreased light levels during the afternoon (14.00-17.00) with respect to the morning (09.00-12.00) are thought to reduce predation pressure on zooplankton by visual predators (Hays, 2003; Gleiss *et al.*, 2013). Motta *et al.* (2010) observed in Cabo Catoche (Mexico) a peak in abundance of whale sharks filter-feeding during mid-morning. On the contrary, Gleiss *et al.* (2013) stated that whale sharks at Ningaloo Reef exhibited ram filter-feeding techniques primarily during sunset and the first hours of night. Thus, pronounced phases of filter-feeding techniques suggested that temporal dynamics of zooplankton aggregation represent critical factors in influencing the behavior of whale sharks in Djibouti.

4.4 Influence of ENSO events on the feeding behaviors and interannual sightings of whale sharks in Djibouti

Beside sea and weather conditions influencing filter-feeding strategies, also the role of the ENSO phenomenon must be taken into consideration both on surface feeding behavior and interannual sightings.

According to Dasari *et al.* (2018), El Niño can lead to a northward shift of the Red Sea Convergence Zone from October to January, altering wind patterns, increasing SSTs and raising rainfall over the Gulf of Aden and southern Red Sea. These changes could affect both whale sharks' gatherings and feeding behavior in Djibouti.

Results showed an attitude of whale sharks to do more A during La Niña and more P or V feeding strategies during El Niño events. However, V and P were the most frequent feeding strategies observed both during El Niño event in 2024 (MEI 2) and La Niña events occurring in 2017 (MEI -0.2), 2020 (MEI -0.2) and 2022 (MEI -0.9). Moreover, the highest number of whale sharks sighted was during El Niño event in 2024 with 33 specimens.

Studies show that during La Niña, trade winds drive stronger currents and warmer temperatures along the coast of Australia enhancing the Leeuwin Current's southward flow and nutrient resuspension, influencing whale shark abundance (Wilson *et al.*, 2001; Sleeman *et al.* 2010). Thus, feeding behaviors and the highest number of whale shark sightings in Djibouti documented during El Niño event, would be possibly due to alternative prey sources favored by warmer SSTs and altered currents not considered in this study.

Recently, Montero-Quintana *et al.* (2021) and Lester *et al.* (2021) reported that *R. typus* can also prey on baitfish using stationary suction-feeding in Bahia de

Los Angeles (Mexico) and Ningaloo Reef, respectively, and Boldrocchi and Bettinetti (2019) reported that juvenile whale sharks attack schools of baitfish in Djibouti. These observations can support the hypothesis that when dense patches of zooplankton are not present, whale sharks do not leave the area. Instead, they adapt by exhibiting flexible feeding behavior strategies on alternative available prey, maximizing their energy gains (Boldrocchi *et al.*, 2019).

It is correct to assume that whale shark distribution and abundance are mainly influenced by productivity and zooplanktonic biomass (Whitehead, 2019; Hachohen-Domené, 2015; Motta, 2010). However, a combination of changing temperatures and prey biomass, driven by oceanographic and atmospheric anomalies (Sequeira, 2012; Sleeman, 2010), can lead whale sharks to shift their foraging behavior and abundance (Jaramillo-Gil, 2021).

5. Conclusions

Studying the effects of environmental changes on whale shark feeding behavior and abundance is challenging, especially due to the lack of information in the literature concerning the topic. This preliminary study demonstrated that chlorophyll-*a* concentration, influenced by other environmental factors, represents a key driver of whale shark feeding behavior. Since whale sharks are highly sensitive to fluctuations in food availability, climate change could have a decisive impact on their feeding ecology and distribution in different hotspot areas. Given the global decline in whale shark populations, understanding how environmental factors influence their feeding behavior and abundance is crucial for assessing their habitat distribution and migration patterns. Therefore, future studies are required for long-term monitoring, as well as implementing and considering other factors to predict their potential roles in shaping feeding behavior, providing more comprehensive insights for conservation efforts.

Current research on whale sharks reveals significant gaps in understanding their behavior and life cycle. Thus, continued investigation into foraging strategies through video surveys, satellite technologies, and photoidentification programs for population assessments is essential. These approaches will not only aid in developing effective management strategies for this species, but also enhance a knowledge of their population dynamics and ecological interactions.

Despite their endangered status, whale sharks still lack adequate protection in many regions, even in seasonal aggregation sites like Djibouti. This highlights the urgent need for global conservation efforts and increased awareness about the threats faced by these filter-feeding sharks.

References

1. Acuña-Marrero, D., Jiménez, J., Smith, F., Hearn, A., Green, J.R., et al. (2014). Whale shark (*Rhincodon typus*) seasonal presence, residence time and habitat use at Darwin Island, Galapagos Marine Reserve. *PLoS One*, 9(12), e115946. DOI: 10.1371/journal.pone.0115946.
2. Afonso, P., McGinty, N., Machete, M. (2014). Dynamics of whale shark occurrence at their fringe oceanic habitat. *PLoS One*, 9(7), e102060. DOI: 10.1371/journal.pone.0102060.
3. Araujo, G., Agustines, A., Tracey, B., Snow, S., Labaja, J., et al. (2019). Photo-ID and telemetry highlight a global whale shark hotspot in Palawan, Philippines. *Scientific Reports*, 9(1), 17209. DOI: 10.1038/s41598-019-53718-w.
4. Arrowsmith, L.M., Sequeira, A.M., Pattiaratchi, C.B., Meekan, M.G. (2021). Water temperature is a key driver of horizontal and vertical movements of an ocean giant, the whale shark *Rhincodon typus*. *Marine Ecology Progress Series*, 679, 101-114. DOI: 10.3354/meps13899.
5. Arzoumanian, Z., Holmberg, J., Norman, B. (2005). An astronomical pattern-matching algorithm for computer-aided identification of whale

- sharks *Rhincodon typus*. *Journal of Applied Ecology*, 42(6), 999-1011. DOI: 10.1111/j.1365-2664.2005.01117.x.
6. Báez, J.C., Barbosa, A.M., Pascual, P., Ramos, M.L., Abascal, F. (2019). Ensemble modeling of the potential distribution of the whale shark in the Atlantic Ocean. *Ecology and Evolution*, 10(1), 175–184. DOI: 10.1002/ece3.5884.
 7. Bava, P., Micarelli, P., Buttino, I. (2022). Zooplankton assemblage diversity in the whale shark *Rhincodon typus* aggregation area of Nosy Be (Madagascar). *Estuarine, Coastal and Shelf Science*, 279(3), 108159. DOI: 10.1016/j.ecss.2022.108159.
 8. Beaugrand, G., Luczak, C., Edwards, M. (2009). Rapid biogeographical plankton shifts in the North Atlantic Ocean. *Global Change Biology*, 15(7), 1790–1803. DOI: 10.1111/j.1365-2486.2009.01848.x.
 9. Becerril-García, E.E., Pancaldi, F., Cruz-Villacorta, A.A., Rivera-Camacho, A.R., Aguilar Cruz, C.A., et al. (2021). General descriptions of the dermis structure of a juvenile whale shark *Rhincodon typus* from the Gulf of California. *Journal of Fish Biology*, 99(4), 1524-1528. DOI: 10.1111/jfb.14827.

10. Berumen, M.L., Braun, C.D., Cochran, J.E., Skomal, G.B., Thorrold, S.R. (2014). Movement patterns of juvenile whale sharks tagged at an aggregation site in the Red Sea. *PLoS ONE*, 9(7), e103536. DOI: 10.1371/journal.pone.0103536.
11. Boldrocchi, G. and Bettinetti, R. (2019). Whale shark foraging on baitfish off Djibouti. *Marine Biodiversity*, 49(4), 2013–2016. DOI: 10.1007/s12526-018-00934-8.
12. Boldrocchi, G., Omar, M., Azzola, A., Bettinetti, R. (2020). The ecology of the whale shark in Djibouti. *Aquatic Ecology*, 54(2), 535–551. DOI: 10.1007/s10452-020-09758-w.
13. Boldrocchi, G., Omar, M., Rowat, D., Bettinetti, R. (2018). First results on zooplankton community composition and contamination by some persistent organic pollutants in the Gulf of Tadjoura (Djibouti). *Science of the Total Environment*, 627, 812–821. DOI: 10.1016/j.scitotenv.2018.01.286.
14. Brooks, K.S., Rowat, D., Pierce, S.J., Jouannet, D., Vely, M. (2010). Seeing spots: photo-identification as a regional tool for whale shark identification. *Western Indian Ocean Journal of Marine Science*, 9(2), 185–194.
15. Cade, D.E., Levenson, J.J., Cooper, R., de la Parra, R., Webb, D.H., Dove, D.M. (2020). Whale sharks increase swimming effort while filter feeding,

- but appear to maintain high foraging efficiencies. *Journal of Experimental Biology*, 223(11), jeb.224402. DOI: 0.1242/jeb.224402.
16. Chen, C.T., Liu, K.M., Joung, S.J. (1997). Preliminary Report on Taiwan's Whale Shark Fishery. *Taipei: TRAFFIC East Asia*, 17(1), 53-57.
 17. Clark, E. and Nelson, D.R. (1997). Young Whale Sharks, *Rhincodon typus*, feeding on a copepod bloom near La Paz, Mexico. *Environmental Biology of Fishes*, 50, 63-73. DOI: 10.1023/A:1007312310127.
 18. Cochran, J.E.M., Kattan, A., Langner, U., Knochel, A.M., Ford, K., Fitzgerald, L., Scott, K., Berumen, M.L. et al. (2024). Fine-scale spatial and temporal trends in Red Sea coral reef research. *Regional Studies in Marine Science*, 71, 103404. DOI: 10.1016/j.rsma.2024.103404.
 19. Colman, J.G. (1997). Review of the biology and ecology of the whale shark. *Journal of Fish Biology*, 51(6), 1219-1234. DOI: 10.1111/j.1095-8649.1997.tb01138.x.
 20. Compagno, L.J.V. (2001). Sharks of the world: an annotated and illustrated catalogue of shark species known to date. *Food and Agriculture Organization of the United Nations*, 2(1).

21. Copping, J.P., Stewart, B.D., McClean, C.J., Hancock, J., Rees, R. (2018). Does bathymetry drive coastal whale shark (*Rhincodon typus*) aggregations? *PeerJ*, 6, e4904. DOI: 10.7717/peerj.4904.
22. Dabar, O.A., Adan, A.B.I., Ahmed, M.M., Awaleh, M.O., Waberi, M.M., Mohamed, J. et al. (2022). Evolution and Trends of Meteorological Drought and Wet Events over the Republic of Djibouti from 1961 to 2021. *Climate*, 10, 148. DOI: 10.3390/cli10100148.
23. Dabar, O.A., Camberlin, P., Pohl, B., Waberi, M.M., Awaleh, M.O., Silah-Eddine, S. (2020). Spatial and temporal variability of rainfall over the Republic of Djibouti from 1946 to 2017. *International Journal of Climatology*, 41, 2729-2748. DOI: 10.1002/joc.6986.
24. Dasari, H.P., Langodan, S., Viswanadhapalli, Y., Vadlamudi, B.R., Papadopoulos, V.P., Hoteit, I. (2016). ENSO influence on the interannual variability of the Red Sea convergence zone and associated rainfall. *International Journal of Climatology*, 38(2), 761-775. DOI: 10.1002/joc.5208.
25. Dasari, H.P., Langodan, S., Viswanadhapalli, Y., Vadlamudi, B.R., Papadopoulos, V.P., Hoteit, I. (2018). ENSO influence on the interannual variability of the Red Sea convergence zone and associated rainfall.

- International Journal of Climatology*, 38(2), 761-775. DOI: 10.1002/joc.5208.
26. de la Parra Venegas, R., Hueter, R., Cano, J.G., Tyminski, J., Gregorio-Remolina, J., Maslanka, M., Ormos, A., Weigt, L., Carlson, B., Alistair, D. (2011). An unprecedented aggregation of whale sharks *Rhincodon typus* in Mexican coastal waters of the Caribbean Sea. *PLoS One*, 6(4), e18994. DOI: 10.1371/journal.pone.0018994.
 27. Di Capua, I., Micarelli, P., Tempesti, J., Reinerio, F.R., Buttino, I. (2021). Zooplankton size structure in the Gulf of Tadjoura (Djibouti) during whale shark sighting: a preliminary study. *Cahiers de Biologie Marine*, 62(3), 290-294. DOI: 10.21411/cbm.a.48866486.
 28. Diamant, S., Pierce, S.J., Rohner, C.A., Graham, R.T., et al. (2021). Population structure, residency, and abundance of whale sharks in the coastal waters off Nosy Be, north-western Madagascar. *Aquatic Conservation: Marine and Freshwater Ecosystems*, 31(12), 3492-3506. DOI: 10.3354/meps13899.
 29. Dove, A.D. and Pierce, S. J. (2022). Whale sharks: Biology, Ecology, and Conservation. *CRC Marine Biology Press*.

30. Dove, A.D.M. (2015). Foraging and ingestive behaviors of whale sharks, *Rhincodon typus*, in response to chemical stimulus cues. *Biology Bulletin*, 228(1), 65-74. DOI: 10.1086/BBLv228n1p65.
31. Duffy, C.A.J. (2002). Distribution, seasonality, lengths, and feeding behavior of whale sharks (*Rhincodon typus*) observed in New Zealand waters. *New Zealand Journal of Marine and Freshwater Research*, 36(3), 565–570. DOI: 10.1080/00288330.2002.9517112.
32. Dulvy, N.K., Rogers, S.I., Jennings, S., Stelzenmuller, V., Dye, S.R., Skjoldal, H.R. (2008). Climate change and deepening of the North Sea fish assemblage: a biotic indicator of warming seas. *Journal of Applied Ecology*, 45, 1029–1039. DOI: 10.1111/j.1365-2664.2008.01488.x.
33. Edwards, K.F., Thomas, M.K., Klausmeier, C.A., Litchman, E. (2016). Phytoplankton growth and the interaction of light and temperature: A synthesis at the species and community level. *Limnology and Oceanography*, 61(4). DOI: 10.1002/lno.10282.
34. Finucci, B., Duffy, C.A.J., Brough, T., Petersen, G., Stephenson, F., et al. (2021). Diver of Spatial Distributions of Basking Shark (*Cetorhinus maximus*) in the Southwest Pacific. *Frontiers in Marine Science*, 8, 2296-7745. DOI: 10.3389/fmars.2021.665337.

35. Fortič, A., Al-Sheikh Rasheed, R., Almajid, Z., Badreddine, A., Báez, J.C., Belmonte-Gallegos, A., Bettoso, N., Borme, D., Camisa, F., Caracciolo, D., et al. (2023). New records of introduced species in the Mediterranean Sea. *Mediterranean Marine Science*, 24(1), 182-202. DOI: 10.12681/mms.34016.
36. Gittings, J.A., Raitsos, D.E., Racault, M.F., Brewin, R.J.W., Pradhan, Y., Sathyendranath, S. Platt, T. (2016). Seasonal phytoplankton blooms in the Gulf of Aden revealed by remote sensing. *Remote Sensing of Environment*, 189, 56-66. DOI: 10.1016/j.rse.2016.10.043.
37. Gleiss, C.A., Wright, S., Liebsch, N., Wilson, P.R., Norman, B. (2013). Contrasting diel patterns in vertical movement and locomotor activity of whale sharks at Ningaloo Reef. *Marine Biology*, 160(11), 29981-29992. DOI: 10.1007/s00227-013-2288-3.
38. Graham, R.T. and Roberts, C.M. (2007). Assessing the size, growth rate and structure of a seasonal population of whale sharks (*Rhincodon typus*, Smith 1828) using conventional tagging and photoidentification. *Fisheries Research*, 84(1), 71-80. DOI: 10.1016/j.fishres.2006.11.026.
39. Gudger, E.W. (1941a). The food and feeding habits of the whale shark *Rhincodon typus*. *J. Elisha Mitchell Science Society*, 57(1), 57–72.

40. Hacoheh-Domené, A., de la Parra-Venegas, R., Dove, A.D.M., Galván-Magaña, F., Galván-Pastoriza, B., Martínez-Rincón, R.O., Cárdenas-Palomo, N. (2015). Habitat suitability and environmental factors affecting whale shark (*Rhincodon typus*) aggregations in the Mexican Caribbean. *Environmental Biology of Fishes*, 98(8), 1953-1964. DOI: 10.1007/s10641-015-0413-5.
41. Han, H., Xiao, R., Gao, G., Yin, B., Liang, S., et al. (2023). Influence of a heavy rainfall event on nutrients and phytoplankton dynamics in a well-mixed semi-enclosed bay. *Journal of Hydrology*, 617, 128932. DOI: 10.1016/j.jhydrol.2022.128932.
42. Hays, G.C. (2003). A review of the adaptive significance and ecosystem consequences of zooplankton diel vertical migrations. *Migration and Dispersal of Marine Organisms: Proceedings of the 37th European Marine Biology Symposium*, 174,163-170.
43. Hoffmayer, E.R., Franks, J.S., Driggers, W.B., Oswald, K.J., Quattro, J.M. (2007). Observations of a feeding aggregation of whale sharks, *Rhincodon typus*, in the north central Gulf of Mexico. *Gulf and Caribbean Research*, 19, 69–73. DOI: 10.18785/ gcr.1902.08.

44. Hsu, H.H., Joung, S.J., Hueter, R.E., Liu, K.M. (2014). Age and growth of the whale shark (*Rhincodon typus*) in the north-western Pacific. *Marine Freshwater Research*, 65, 1145–1154. DOI: 10.1071/mf13330.
45. Jaramillo-Gil, S., Pardo, M.A., Vázquez-Haikin, A., Bolaños-Jiménez, J., Sosa Nishizaki, O. (2023). Whale shark abundance forecast: the interannual hotspot effect. *Journal of Applied Ecology*, 60(6), 954–966. DOI: 10.1111/1365-2664.14406.
46. Legaspi, C., Miranda, J., Labaja, J., Snow, S., Ponzio, A., et al. (2020). In-water observations highlight the effects of provisioning on whale shark behavior at the world's largest whale shark tourism destination. *Royal Society Open Science*, 7(12), 200392. DOI: 10.1098/RSOS.200392.
47. Lester, E.K., Langlois, T.J., McCormick, M.I., Simpson, S.D., Bond, T., Meekan, M.G. (2021). Relative influence of predators, competitors and seascape heterogeneity on behaviour and abundance of coral reef mesopredators. *Nordic Society Oikos*, 130(12), 2239-2249. DOI: 10.1111/oik.08463.
48. Manuhutu, J.F., Wiadnya, D.G.R., Sambah, A.B., Herawati, E.Y. (2021). The presence of whale sharks based on oceanographic variations in Cenderawasih Bay National Park, Papua, Indonesia. *Biodiversitas Journal*

- of Biological Diversity*, 22(11), 4948-4955. DOI: 10.13057/biodiv/d221129.
49. Marliana, S.N., Bataona, M., Ihsan, E.N. (2018). Zooplankton communities in Cenderawasih Bay National Park, West Papua: can their composition be used to predict whale shark *Rhincodon typus* (Smith, 1828) appearance frequencies? *Earth and Environmental Science*, 139(1), 012012. DOI: 10.1088/1755-1315/139/1/012012.
50. Marsili, L., Consales, G., Romano, P., Rosai, R., Bava, P., Reinerio, F.R., Micarelli, P. (2023). A Cocktail of Plankton and Organochlorines for Whale Shark in the Foraging Areas of Nosy Be (Madagascar). *Diversity*, 15(8), 911. DOI: 10.3390/d15080911.
51. Martin, R.A. (2007). A review of behavioral ecology of whale sharks (*Rhincodon typus*). *Fisheries Research*, 84(1), 10-16. DOI: 10.1016/j.fishres.2006.11.010.
52. Martino, C., Morton, J.T., Marotz, C.A., Thompson, L.R., Tripathi, A., et al. (2019). A Novel Sparse Compositional Technique Reveals Microbial Perturbations. *MSystems*, 4(1), 00016-19. DOI: 10.1128/msystems.
53. Matsumoto, R., Matsumoto, Y., Ueda, K., Suzuki, M., Asahina, K., Sato, K. (2017). Sexual maturation in a male whale shark (*Rhincodon typus*) based

- on observations made over 20 years of captivity. *Academic Journal*, 117(1), 78. DOI: 10.7755/FB.117.1-2.9
54. Meekan, M.G., Fuiman, L.A., Davis, R., Berger, Y., Thums, M. (2015). Swimming strategy and body plan of the world's largest fish: implications for foraging efficiency and thermoregulation. *Frontiers in Marine Science*, 2, 64. DOI: 10.3389/fmars.2015.00064.
55. Meekan, M.G., Taylor, B.M., Lester, E., Sequeira, A.M.M., Dove, D.M., Thums, M. et al. (2020). Asymptotic growth of whale sharks suggests sex-specific life-history strategies. *Frontiers in Marine Science*, 7, 575683. DOI: 10.3389/fmars.2020.575683.
56. Micarelli, P., Romano, C., Buttino, I., Reinerio, F., Serangeli, C., Sperone, E. (2017). Phytoplankton bloom and seasonal presence of whale shark (*Rhincodon typus*) along the coast of Djibouti – Gulf of Aden. *International Journal of Current Advanced Research*, 6(5), 3948-3949. DOI: 10.24327/ijcar.2017.3949.0403.
57. Montero-Quintana, A.N., Ocampo-Valdez, C.F., Vázquez - Haikin, J.A., Sosa-Nishizaki, O., Osorio-Beristain, M. (2021). Whale Shark (*Rhincodon typus*) predatory flexible feeding behaviors on schooling fish. *Journal of Ethology*, 39(2), 399-410. DOI: 10.1007/s10164-021-00717-y.

58. Motta, P.J., Maslanka, M., Hueter, R.E., Davis, R.L., de la Parra, R., et al. (2010). Feeding anatomy, filter-feeding rate, and diet of whale sharks *Rhincodon typus* during surface ram filter feeding off the Yucatan Peninsula, Mexico. *Zoology*, 113(4), 199-212. DOI: 10.1016/j.zool.2009.12.001.
59. Nelson, J. and Eckert, S. (2007). Foraging ecology by whale sharks (*Rhincodon typus*) within Bahia de Los Angeles, Baja California Norte, Mexico. *Fisheries Research*, 84, 47–64. DOI: 10.1016/j.fishres.2006.11.013.
60. Norman, B. (2002). Review of current and historical research on the ecology of whale sharks (*Rhincodon typus*), and applications to conservation through management of the species. Unpublished report for the *WA Department of Conservation and Land Management, Perth*.
61. Norman, B. M. and Stevens, J. D. (2007). Size and maturity status of the whale shark (*Rhincodon typus*) at Ningaloo Reef in Western Australia. *Fisheries Research*, 84, 81–86. DOI: 10.1016/j.fishres.2006.11.015.
62. Omar, Y.M., Mémery, L., Carton, X., Daher, A., Duviolbourg, E. (2016). Effects of Monsoon Winds and Topographical Features on the Vertical Thermohaline and Biogeochemical Structure in the Gulf of Tadjourah

- (Djibouti). *Open Journal of Marine Science*, 6(3), 440-445. DOI: 10.4236/ojms.2016.63037.
63. Osgood, G.J., White, E.R., Baum, J.K. (2020). Effect of climate-change-driven gradual and acute temperature changes on shark and ray species. *Journal of Animal Ecology*, 90, 2547-2559. DOI: 10.1111/1365-2656.13560.
64. Paig-Tran, E.W. and Summers, A.P. (2014). Comparison of the structure and composition of the branchial filters in suspension feeding elasmobranchs. *The Anatomical Record*, 297(4), 701-715. DOI: 10.1002/ar.22850.
65. Pierce, S.J. and Norman, B. (2016). The IUCN Red List of Threatened Species 2016. *IUCN*: Gland, Switzerland.
66. Pierce, S.J., Rohner, C.A., Matsumoto, R., Pardo, S.A., Meekan, M.G., et al. (2021). Whale shark reproduction, growth, and demography. *Whale sharks: Biology, ecology and conservation*, 2, 13-45.
67. Ramírez-Macías, D., Vázquez-Haikin, A., Vázquez-Juárez, R. (2012). Whale shark *Rhincodon typus* populations along the west coast of the Gulf of California and implications for management. *Endangered Species Research*, 18(2), 115-128. DOI: <https://doi.org/10.3354/esr00437>.

68. Ranintyari, M., et al. (2018). Effects of oceanographic factors on spatial distribution of Whale Shark in Cendrawasih Bay National Park, West Papua. *Earth Environmental Science*, 149(1), 012050. DOI: 10.1088/1755-1315/149/1/012050.
69. Riley, M.J., Hale, M.S., Harman, A., Rees, R.G. (2010), Analysis of whale shark *Rhincodon typus* aggregations near South Ari Atoll, Maldives Archipelago. *Aquatic Biology*, 8(2), 145–150. DOI: 10.3354/ab00215.
70. Robinson, D.P., Jaidah, Y.M., Bach, S.S., Rohner, C.A., Jabado, W.R., et al. (2017). Some like it hot: repeat migration and residency of whale sharks within an extreme natural environment. *PLoS One*, 12(9), e0185360. DOI: 10.1371/journal.pone.0185360.
71. Rohner, C.A. and Prebble, C.E. (2021). Whale shark foraging, feeding, and diet. *Whale sharks: Biology, Ecology, and Conservation*, 1, 153-180.
72. Rohner, C.A., Anthony, J.R., Jaine, R.A., Bennett, M.B., Weeks, S.J., Cliff, G., Robinson, D.P., Reeve-Arnold, K.E., Pierce, S.J. (2017). Satellite tagging highlights the importance of productive Mozambican coastal waters to the ecology and conservation of whale sharks. *PeerJ*, 6(6), e4161. DOI: 10.7717/peerj.4161.

73. Rohner, C.A., Armstrong, A.J., Pierce, S.J., Prebble, C.E., Cagua, E.F., Cochran, J.E., Berumen, M.L., Richardson, A.J. (2015). Whale sharks target dense prey patches of sergestid shrimp off Tanzania. *Journal of Plankton Research*, 37(2), 352-362. DOI: 10.1093/plankt/fbv010.
74. Rohner, C.A., et al. (2015). Laser photogrammetry improves size and demographic estimates for whale sharks. *PeerJ*, 3, e886. DOI: 10.7717/peerj.886.
75. Rohner, C.A., Pierce, S.J., Marshall, A.D., Weeks, S.J., Bennett, M.B., Richardson, A.J. (2013). Trends in sightings and environmental influences on a coastal aggregation of manta rays and whale sharks. *Marine Ecology Progress Series*, 482, 153-168. DOI: 10.3354/meps10290.
76. Rowat, D. and Brooks, K.S. (2012). A review of the Biology, Fisheries and Conservation of the Whale Shark *Rhincodon typus*. *Journal of Fish Biology*, 80(5), 1019-1056. DOI: 10.1111/j.1095-8649.2012.03252.x.
77. Rowat, D., Brooks, K., March, A., McCarten, C., Jouannet, D., Riley, L., Gareth, J., Morgan, P., Vely, M., Bruno, P. (2011). Long-term membership of whale sharks (*Rhincodon typus*) in coastal aggregations in Seychelles and Djibouti. *Marine and Freshwater Research*, 62, 621-627. DOI: 10.1071/MF10135.

78. Rowat, D., Gore, M., Meekan, M.G., Lawler, I.R., Bradshaw, J.A. (2008). Aerial survey as a tool to estimate whale shark abundance trends. *Journal of Experimental Marine Biology and Ecology*, 368, 1-8. DOI: 10.1016/j.jembe.2008.09.001.
79. Rowat, D., Leblond, S.T., Pardigon, B., Vely, M., Jouannet, D., Webster, I.A. (2016). Djibouti-a kindergarten for whale sharks? *QScience In: Proceedings of the 4th international whale shark conference*. DOI: 10.5339/qproc.2016.iwsc4.54.
80. Rowat, D., Meekan, M.G., Engelhardt, U., Pardigon, B., Vely, M. (2007). Aggregations of juvenile whale sharks (*Rhincodon typus*) in the Gulf of Tadjoura, Djibouti. *Environmental Biology of Fishes*, 80(4), 465–472. DOI: 10.1007/s10641-006-9148-7.
81. Rowat, D., Speed, C.W., Meekan, M.G., Gore, M.A., Bradshaw, C.J.A. (2009). Population abundance and apparent survival of the vulnerable whale shark *Rhincodon typus* in the Seychelles aggregation. *Oryx*, 43(4), 591-598. DOI:10.1017/S0030605309990408.
82. Ryan, J.P., Kudela, R.M., Birch, J.M., Bowers, H.A., Chavez, F.P., Doucette, G.J., Smith, G.J. et al. (2017). Causality of an extreme harmful algal bloom in Monterey Bay, California, during the 2014-2016 northeast

- Pacific warm anomaly. *Geophysical Research Letters*, 44(11), 5571-5579.
DOI: 10.1002/2017GL072637.
83. Saji, N.H., Goswami, B.N., Vinayachandran, P.N., Yamagata, T. (1999). A dipole mode in the tropical Indian Ocean. *Nature*, 401(6751), 360-363. DOI: 10.1038/43854.
84. Salem Abado, F. (1990). El-Niño et la variabilité des précipitations dans la République de Djibouti. *Revue de l'ISERST, Sciences & techniques*, 4, 19–30.
85. Schlaff, A.M., Heupel, M.R., Simpfendorfer, C.A. (2014). Influence of environmental factors on shark and ray movement, behaviour and habitat use: A review. *Fish Biology and Fisheries* 24, 1089-1103. DOI: 10.1007/s11160-014-9364-8.
86. Sequeira, A., Mellin, C., Meekan, M.G., Fordham, D.A., Bradshaw, C.J. (2014). Predicting current and future global distributions of whale sharks. *Global Change Biology*, 20(3), 778-789. DOI:10.1111/gcb.12343.
87. Sequeira, A., Mellin, C., Meekan, M.G., Sims, D.W., Bradshaw, C.J.A. (2013). Inferred global connectivity of whale shark *Rhincodon typus* population. *Journal of Fish Biology*, 82(2), 367- 389. DOI:10.1111/jfb.12017.

88. Sequeira, A., Mellin, C., Rowat, D., Meekan, M., Bradshaw, C. (2012). Ocean-scale prediction of whale shark distribution. *Diversity and Distributions*, 18, 504-518. DOI:10.1111/j.1472-4642.2011.00853.x.
89. Sims, D.W. and Quayle, V.A. (1998). Selective foraging behaviour of basking sharks on zooplankton in a small-scale front. *Nature*, 393(6684), 460-464. DOI: 10.1038/30959.
90. Siswanto, E. (2020). Temporal variability of satellite-retrieved chlorophyll-*a* data in Arctic and subarctic ocean regions within the past two decades. *International Journal of Remote Sensing*, 41(19), 7427–7445. DOI: 10.1080/01431161.2020.1759842.
91. Sleeman, J.C., Meekan, M.G., Wilson, S.G., Polovina, J.J, Stevens, J.D., Bogg, G.S., Bradshaw, J.A. (2010). To go or not to go with the flow: Environmental influences on whale sharks movement patterns. *Journal of Experimental Marine Biology and Ecology*, 390(10), 84-89. DOI: 10.1016/j.jembe.2010.05.009.
92. Speed, C.W., Meekan, M.G., Bradshaw, C.J.A. (2007) Spot the match wildlife photo- identification using information theory. *Frontiers in Zoology*, 4(2). DOI: 10.1186/1742-9994-4-2.

93. Speed, C.W., Meekan, M.G., Rowat, D., Pierce, S.J., Marshall, A.D., Bradshaw, C.J.A. (2008). Scarring patterns and relative mortality rates of Indian Ocean whale sharks. *Journal of Fish Biology*, 72(6), 1488- 1503. DOI: 10.1111/j.1095-8649.2008.01810.x.
94. Squire, J.L. (1990). Distribution and apparent abundance of the basking shark, *Cetorhinus maximus*, off the central and southern California coast, 1962-85. *Marine Fisheries Review*, 52(2), 8-11.
95. Taylor, G. (2007). Ram filter-feeding and nocturnal feeding of whale sharks (*Rhincodon typus*) at Ningaloo Reef, Western Australia. *Fisheries Research*, 84(1), 65-70. DOI: 10.1016/j.fishres.2006.11.014.
96. Tomita, T., Toda, M., Murakumo, K., Miyamoto, K., Matsumoto, R., Ueda, K., Sato, K. (2021). Volume of the whale shark and their mechanism of vertical feeding. *Zoology*, 147, 125932. DOI: 10.1016/j.zool.2021.125932.
97. Towner, A.V., Underhill, L.G., Jewell, O.J.D., Smale, M.J. (2013). Environmental Influences on the Abundance and Sexual Composition of White Sharks *Carcharodon carcharias* in Gansbaai, South Africa. *PLoS ONE*, 8(8), e71197. DOI: 10.1371/journal.pone.0071197.
98. Turan, C., Gürlek, M., Ergüden, D., Kabasakal, H. (2021). A new record for the shark fauna of the Mediterranean Sea: Whale shark *Rhincodon typus*

- (Orectolobiformes: Rhincodontidae). In *Annales: Series Historia Naturalis*, 31(2), 167-172. DOI: 10.19233/ASHN.2021.20.
99. Turnbull, S.D. and Randell, J.E. (2006). Rare occurrence of a *Rhincodon typus* (whale shark) in the Bay of Fundy, Canada. *Northeastern Naturalist*, 13, 57–58. DOI: 10.1656/1092-6194(2006)13[57:ROOART]2.0.CO;2.
100. Tyminski, J.P., de la Parra-Venegas, R., González-Cano, J., Hueter, R.E. (2015). Vertical movements and behavior of whale sharks as revealed by pop-up satellite tags in the eastern Gulf of Mexico. *PLoS One*, 10(11), e0142156. DOI: 10.1371/journal.pone.0142156.
101. Van Tienhoven, A.M., Den Hartog, J.E., Reijns, R., Peddemors, V.M. (2007). A computer- aided program for pattern-matching of natural marks of the spotted ragged tooth shark *Carcharias taurus* (Rafinesque, 1810). *Journal of Applied Ecology*, 44(2), 273–280. DOI: 10.1111/j.1365-2664.2006.01273.x.
102. Wearmouth, V.J. and Sims, D.W. (2008). Sexual segregation in marine fish, reptiles, birds and mammals: behaviour patterns, mechanisms and conservation implications. *Advances in Marine Biology* 54,107–170. DOI: 10.1016/S0065.

103. Whitehead, D.A., Pancaldi, F., Jakes-Cota, U., Galván-Magaña, F., González-Armas, R. (2020). The influence of zooplankton communities on the feeding behavior of whale shark in Bahia de La Paz, Gulf of California. *Revista Mexicana de la Biodiversidad*, 91, e913054. DOI: 10.22201/ib.20078706e.2020.91.3054.
104. Wilson, S.G., Taylor, J.G., Pearce, A.F. (2001). The seasonal aggregation of whale sharks at Ningaloo Reef, Western Australia: currents, migrations and the El Niño/Southern Oscillation. *Environmental Biology of Fishes*, 61, 1-11. DOI: 10.1023/A:1011069914753.
105. Wolter, K. and Timlin, M.S. (2011). El Niño/Southern Oscillation behavior since 1871 as diagnosed in an extended multivariate ENSO index. *International Journal of Climatology*, 31, 1074–1087. DOI: 10.1002/joc.2336.
106. Womersley, F.C., Humphries, N.E., Queiroz, N., Vedor, M., Furtado, M., et al. (2022). Global collision-risk hotspot of marine traffic and the world's largest fish, the whale shark. *Proceedings of the National Academy of Sciences of the United States of America*, 119(20), e2117440119. DOI: 10.1073/pnas.2117440119.

Photos bibliography

- Figure 1: photo by Andrea Izzotti.
- Figure 2: Rowat, D. and Brooks, K.S. (2012). A review of the Biology, Fisheries and Conservation of the Whale Shark *Rhincodon typus*. *Journal of Fish Biology*, 80(5), 1019- 1056. DOI: 10.1111/j.1095-8649.2012.03252.x.
- Figure 5, 12: photo by Rebecca Squadroni, Djibouti 2024.
- Figure 6: Boldrocchi, G., Robinson, D., Omar, M., Schmidt, J.V. et al. (2023). Annual Recurrence of the Critically Endangered Bowmouth Guitarfish (*Rhina ancylostomus*) in Djibouti Waters. *Biology*, 12(10), 1302. DOI: 10.3390/biology12101302.
- Figure 7, 8, 9, 10, 11, 13: photo by Sharks Studies Center.

Sitography

- <https://climateknowledgeportal.worldbank.org/home>
- <https://oceanservice.noaa.gov/facts/ninonina.html>
- <https://psl.noaa.gov/enso/mei.old/mei.html>
- <https://www.copernicus.eu/en>

- <https://www.windguru.cz/4910>

Photos sitography

- Figure 3: <https://www.sharkguardian.org>
- Figure 4: <https://www.nationalgeographic.com>

Acknowledgements

Vorrei riservare questo spazio finale della mia tesi di laurea ai ringraziamenti verso tutti coloro che hanno contribuito, con il loro instancabile supporto, alla realizzazione della stessa.

In primis desidero ringraziare la mia relattrice, la Prof.ssa Emanuela Fanelli, per i suoi preziosi consigli e per la sua disponibilità. In particolare, la ringrazio per avermi trasmesso l'importanza di un approccio olistico al lavoro di ricerca. La sua guida mi ha aiutato a sviluppare una prospettiva critica e mi ha permesso di acquisire una visione più completa sulla stesura dell'elaborato.

Un doveroso e sincero ringraziamento va alla mia relattrice esterna, la Dott.ssa Francesca Romana Reinero, oltre che al Dott. Primo Micarelli e a tutto il team del Centro Studi Squali. Considero una grande fortuna aver potuto realizzare il mio lavoro di tesi in un contesto così stimolante e dinamico, che mi ha offerto l'opportunità di mettermi alla prova e acquisire un'esperienza di inestimabile valore per le mie aspirazioni future.

Un pensiero speciale va alla mia famiglia allargata, che è sempre stata per me un porto sicuro in un mare in tempesta. Grazie per aver creduto sempre in me e per aver incoraggiato i miei sogni e le mie ambizioni, stando sempre al mio fianco.

Infine, ringrazio tutti i miei amici, per la loro comprensione e il loro supporto.

Grazie per avermi ascoltato, spronato e per aver condiviso con me gioie e difficoltà... ma soprattutto per aver imparato la differenza tra polipo e polpo!

Rebecca